

Chapter 7

Ceramic Matrix Composites

Ceramic materials in general have a very attractive package of properties: high strength and high stiffness at very high temperatures, chemical inertness, low density, and so on. This attractive package is marred by one deadly flaw, namely, an utter lack of toughness. They are prone to catastrophic failures in the presence of flaws (surface or internal). They are extremely susceptible to thermal shock and are easily damaged during fabrication and/or service. It is therefore understandable that an overriding consideration in ceramic matrix composites (CMCs) is to toughen the ceramics by incorporating fibers in them and thus exploit the attractive high-temperature strength and environmental resistance of ceramic materials without risking a catastrophic failure. It is worth pointing out at the very outset that there are certain basic differences between CMCs and other composites. The general philosophy in nonceramic matrix composites is to have the fiber bear a greater proportion of the applied load. This load partitioning depends on the ratio of fiber and matrix elastic moduli, E_f/E_m . In nonceramic matrix composites, this ratio can be very high, while in CMCs, it is rather low and can be as low as unity; think of alumina fiber reinforced alumina matrix composite. Another distinctive point regarding CMCs is that because of limited matrix ductility and generally high fabrication temperature, thermal mismatch between components has a very important bearing on CMC performance. The problem of chemical compatibility between components in CMCs has ramifications similar to those in, say, MMCs. We first describe some of the processing techniques for CMCs, followed by a description of some salient characteristics of CMCs regarding interface and mechanical properties and, in particular, the various possible toughness mechanisms, and finally a description of some applications of CMCs.

7.1 Processing of CMCs

Ceramic matrix composites (CMCs) can be processed either by conventional powder processing techniques used for making polycrystalline ceramics or by some new techniques developed specifically for making CMCs. We describe below some of the important processing techniques for CMCs.

7.1.1 Cold Pressing and Sintering

Cold pressing of the matrix powder and fiber followed by sintering is a carryover from conventional processing of ceramics. Generally, in the sintering step, the matrix shrinks considerably and the resulting composite has many cracks. In addition to this general problem of shrinkage associated with sintering of any ceramic, certain other problems arise when we put high-aspect ratio (length/diameter) reinforcements in a glass or ceramic matrix material and try to sinter. Fibers and whiskers can form a network that may inhibit the sintering process. Depending on the difference in thermal expansion coefficients of the reinforcement and matrix, a hydrostatic *tensile* stress may develop in the matrix on cooling, which will counter the driving force (surface energy minimization) for sintering (Raj and Bordia 1989; Kellett and Lange 1989). Thus, the densification rate of the matrix will, in general, be retarded in the presence of reinforcements (Bordia and Raj 1988; De Jonghe et al. 1986; Sacks et al. 1987; Rahaman and De Jonghe 1987; Prewo 1986). Whiskers or fibers may also give rise to the phenomenon of bridging, which is a function of the orientation and aspect ratio of the reinforcement.

7.1.2 Hot Pressing

Some form of hot pressing is frequently resorted to in the consolidation stage of CMCs. This is because a simultaneous application of pressure and high temperature can accelerate the rate of densification and a pore-free and fine-grained compact can be obtained. A common variant, called the *slurry infiltration* process, is one of the most important techniques used to produce continuous fiber reinforced glass and glass-ceramic composites (Sambell et al. 1974; Phillips 1983; Cornie et al. 1986; Prewo and Brennan 1980; Brennan and Prewo 1982; Chawla et al. 1993a, b). The slurry infiltration process involves two stages:

1. Incorporation of a reinforcing phase into an unconsolidated matrix.
2. Consolidation of matrix by hot pressing.

Figure 7.1 shows a schematic of this process. In addition to incorporation of the reinforcing phase, the first stage involves some kind of fiber alignment. A fiber tow

or a fiber preform is impregnated with matrix-containing slurry by passing it through a slurry tank. The impregnated fiber tow or preform sheets are similar to the prepregs used in polymer matrix composites. The slurry consists of the matrix powder, a carrier liquid (water or alcohol), and an organic binder. The organic binder is burned out prior to consolidation. Wetting agents may be added to ease the infiltration of the fiber tow or preform. The impregnated tow or prepreg is wound on a drum and dried. This is followed by cutting and stacking of the prepregs and consolidation in a hot press. The process has the advantage that, as in PMCs, the prepregs can be arranged in a variety of stacking sequences, e.g., unidirectional, cross-plyed ($0^\circ/90^\circ/0^\circ/90^\circ$, etc.), or angle-plyed ($+\theta^\circ/-\theta^\circ/+\theta^\circ/-\theta^\circ$, etc.). Figure 7.2a shows an optical micrograph of a transverse section of a unidirectional Nicalon fiber/glass matrix composite. In general, such glass matrix composites are well consolidated, i.e., there is hardly any porosity. Porosity can be a problem with crystalline ceramics. Figure 7.2b shows the pressure and temperature schedule used during hot pressing of a typical CMC.

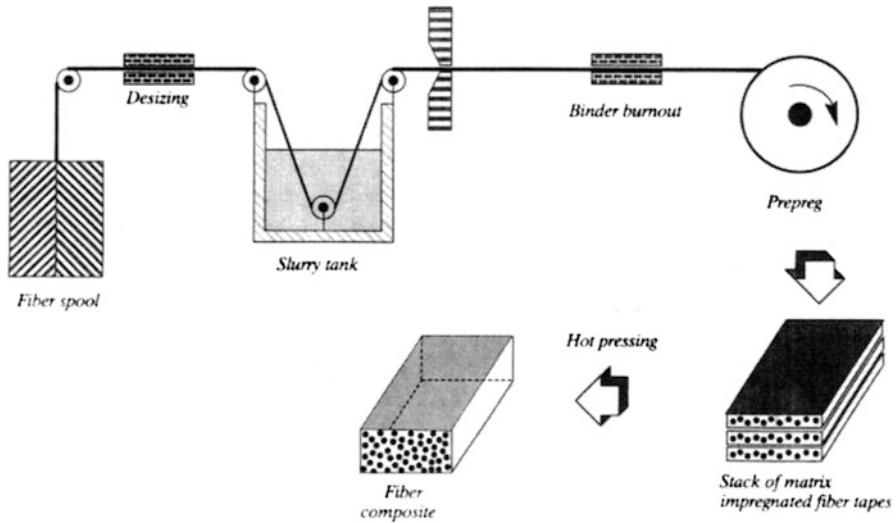


Fig. 7.1 Schematic of the slurry impregnation process

The slurry infiltration process is well suited for glass or glass–ceramic matrix composites, mainly because the processing temperatures for these materials are lower than those used for crystalline matrix materials and glassy phase has good flow properties. Any hot pressing process has certain limitations in producing complex shapes. The fibers should suffer little or no damage during handling. Application of a very high pressure can easily damage fibers. Refractory particles of a crystalline ceramic can damage fibers by mechanical contact. The reinforcement can also suffer damage from reaction with the matrix at very high processing temperatures. The matrix should have as little porosity as possible in the final product as porosity in a

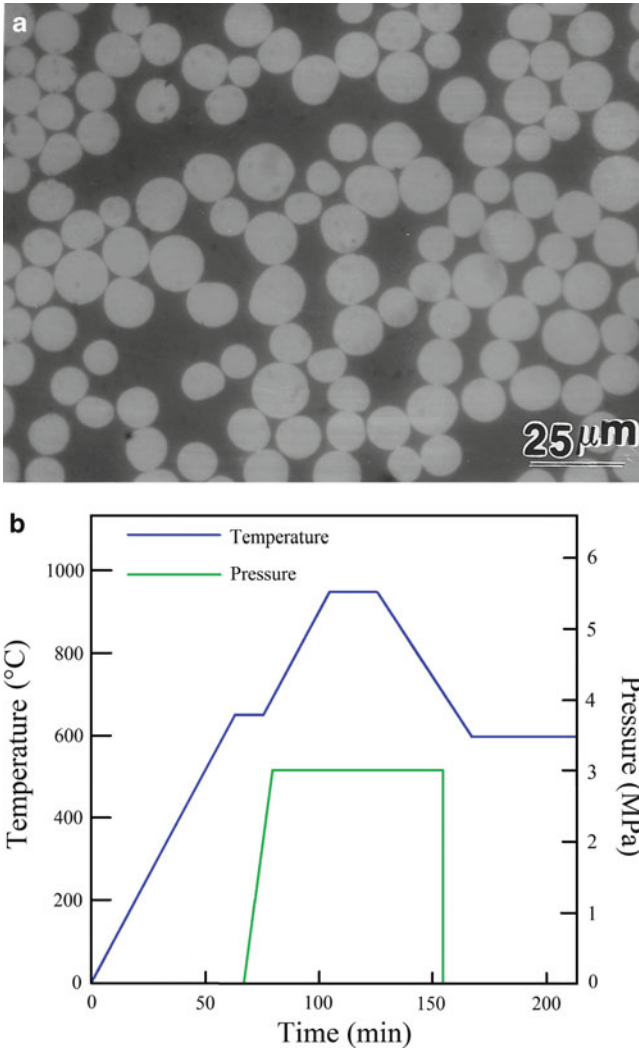


Fig. 7.2 (a) An optical micrograph of a transverse section of a unidirectional Nicalon fiber/glass matrix composite. (b) Pressure and temperature schedule used during hot pressing of a typical composite

structural ceramic material is highly undesirable. To this end, it is important to completely remove the fugitive binder and use a matrix powder particle smaller than the fiber diameter. The hot pressing operational parameters are also important. Precise control within a narrow working temperature range, minimization of the processing time, and utilization of a pressure low enough to avoid fiber damage are important factors in this final consolidation part of the process. Fiber damage and any fiber/matrix interfacial reaction, along with its detrimental effect on the bond strength, are unavoidable attributes of the hot pressing operation.

In summary, the slurry infiltration process generally results in a fairly uniform fiber distribution; low porosity and high strength values can be obtained. The main disadvantage of this process is that one is restricted to relatively low melting or low softening point matrix materials.

Whisker reinforced CMCs are generally made by mixing the whiskers with a ceramic powder slurry, followed by drying and hot-pressing. Sometimes hot isostatic pressing (HIPing) rather than uniaxial hot pressing is used. Whisker agglomeration in a green body is a major problem. Mechanical stirring and adjustment of pH level of the suspension (matrix powder + whiskers in water) can be of help in this regard. Addition of whiskers to slurry can result in very high viscosity. Also, whiskers with large aspect ratios (>50) tend to form bundles and clumps (Liu et al. 1991). Obtaining well-separated and deagglomerated whiskers is of great importance for reasonably high-density composites. Use of organic dispersants (Barclay et al. 1987), techniques such as agitation mixing assisted by an ultrasonic probe, and deflocculation by a proper pH control (Yang and Stevens 1990) can be usefully employed. Most whisker reinforced composites are made at temperatures in the 1,500–1,900°C range and pressures in the 20–40 MPa range (Homeny et al. 1987; Shalek et al. 1986).

7.1.3 Reaction Bonding Processes

Reaction bonding processes similar to the ones used for monolithic ceramics can be used to make ceramic matrix composites. Reaction bonding process has the following advantages:

- Problems with matrix shrinkage during densification can be avoided.
- Rather large volume fractions of whiskers or fiber can be used.
- Multidirectional, continuous fiber preforms can be used.
- The reaction bonding temperatures for most systems are generally lower than the sintering temperatures so that fiber degradation can be avoided.

One great disadvantage of this process is that high porosity is difficult to avoid.

A hybrid process involving a combination of hot pressing and reaction bonding technique can also be used (Bhatt 1986; Bhatt 1990). A silicon cloth is prepared by attrition milling a mixture of silicon powder, a polymer binder, and an organic solvent to obtain a dough of proper consistency. This dough is then rolled to make a silicon cloth of desired thickness. Fiber mats are made by filament winding of silicon carbide with a fugitive binder. The fiber mats and silicon cloth are stacked in an alternate sequence, debinderized (the step of binder removal), and hot pressed in a molybdenum die in a nitrogen or vacuum environment. The temperature and pressure are adjusted to produce a handleable preform. At this stage, the silicon matrix is converted to silicon nitride by transferring the composite to a nitriding furnace between 1,100 and 1,400°C. Typically, the silicon nitride matrix has about 30% porosity, which is not unexpected in reaction bonded silicon nitride.

Reaction bonding processing can also be used to make oxide fiber/oxide matrix composites, which are very attractive for high temperature applications in air. Specifically, the technique has been applied to alumina (Claussen et al. 1989, 1994; Kristofferson et al. 1993) and mullite (Wu and Claussen 1994) systems. Mullite is an important technological ceramic that forms as an intermediate phase in the $\text{SiO}_2\text{-Al}_2\text{O}_3$ system. The chemical composition of mullite is commonly denoted as $3\text{Al}_2\text{O}_3\cdot 2\text{SiO}_2$ (which corresponds to 60 mol% Al_2O_3), in reality, it refers to a solid solution in the range of 60–63 mol% Al_2O_3 below 1,600°C (Schneider and Komarneni 2005). In the case of producing an oxide matrix in a preform of oxide fibers, reaction bonding process involves direct oxidation of starting powders to create the matrix. The process has a shorter processing time than forming matrix by infiltration techniques. For the case of alumina, a starting powder consisting of Al- Al_2O_3 or a slurry infiltrated compact is heat treated in an oxidizing atmosphere. The aluminum powder oxidizes to Al_2O_3 . But the key point is that in this process of oxidation, there occurs a 28% volume expansion which partially compensates for the sintering shrinkage. Oxidation is usually completed below 1,100°C, where sintering does not take place. Mullite matrix can be obtained by adding SiC to the starting powder, which is then oxidized during processing to form the SiO_2 component. An alternative technique of producing mullite involves the use of an Al-Si alloy as a starting material. Because problems with shrinkage during densification are avoided, reaction bonding is an attractive and fast method of producing fiber reinforced, ceramic composites.

7.1.4 Infiltration

Infiltration of a preform made of reinforcement can be done with a matrix material in solid, liquid, or gaseous form.

7.1.4.1 Liquid Infiltration

This technique is very similar to liquid polymer or liquid metal infiltration (Fig. 7.3). Proper control of the fluidity of the liquid matrix is, of course, the key to this technique. It yields a high-density matrix, i.e., no pores in the matrix. Almost any reinforcement geometry can be used to produce a virtually flaw-free composite. The temperatures involved, however, are much higher than those encountered in polymer or metal processing. Processing at such high temperatures can lead to deleterious chemical reactions between the reinforcement and the matrix. Thermal expansion mismatch between the reinforcement and the matrix, the rather large temperature interval between the processing temperature and room temperature, and the low strain to failure of ceramics can add up to a formidable set of problems in producing a crack-free CMC. Viscosities of ceramic melts are generally quite high, which makes the infiltration of preforms rather difficult. Wettability of the

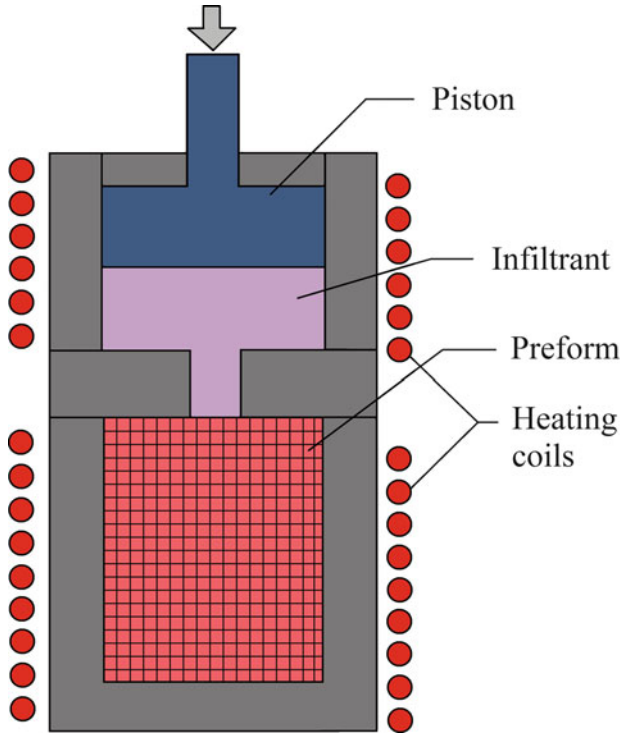


Fig. 7.3 Schematic of the melt infiltration process [after Cornie et al. (1986), used with permission]

reinforcement by the molten ceramic is another item to be considered. Hillig (1988) has discussed the melt infiltration processing of ceramic matrix composites in regard to chemical reactivity, melt viscosity, and wetting of the reinforcement by the melt. A preform made of reinforcement in any form (for example, fiber, whisker, or particle) having a network of pores can be infiltrated by a ceramic melt by using capillary pressure. Application of pressure or processing in vacuum can aid in the infiltration process. Assuming that the preform consists of a bundle of regularly spaced, parallel channels, one can use Poiseuille's equation to obtain the infiltration height, h :

$$h = \sqrt{\frac{\gamma r t \cos \theta}{2\eta}},$$

where r is the radius of the cylindrical channel, t is the time, γ is the surface energy of the liquid infiltrant, θ is the contact angle of wetting, and η is the viscosity. The penetration height is proportional to the square root of time, and the time required to

penetrate a given height is inversely proportional to the viscosity of the melt. Penetration will also be easier if the contact angle is low (i.e., better wettability), and the surface energy, γ , and the pore radius, r , are large. If the radius, r , of the channel is made too large, the capillarity effect will be lost.

Infiltration of a fibrous preform by a molten intermetallic matrix material under pressure has been successfully done (Nourbakhsh and Margolin 1990). Alumina fiber reinforced intermetallic matrix composites (e.g., TiAl, Ni₃Al, and Fe₃Al matrix materials) have been prepared by *pressure casting*, also called *squeeze casting* (Nourbakhsh and Margolin 1990; Nourbakhsh et al. 1990). The matrix alloy is melted in a crucible in a vacuum while the fibrous preform is heated separately. The molten matrix material (at about 100°C above the melting temperature, T_m) is poured onto the fibers and argon gas is introduced simultaneously. Argon gas pressure forces the melt to infiltrate the preform. The melt generally contains additives to aid wetting of the fibers.

We may summarize the advantages and disadvantages of different melt infiltration techniques as follows. The advantages are as follows:

- The matrix is formed in a single processing step.
- A homogeneous matrix can be obtained.

The disadvantages of infiltration techniques are as follows:

- High melting points of ceramics mean a greater likelihood of reaction between the melt and the reinforcement.
- Ceramics have higher melt viscosities than metals; therefore, infiltration of preforms is relatively difficult.
- The matrix is likely to crack because of the differential shrinkage between the matrix and the reinforcement on solidification. This can be minimized by choosing components with nearly equal coefficients of thermal expansion.

7.1.5 Directed Oxidation or the Lanxide™ Process

Yet another version of liquid infiltration is the directed oxidation process, or the Lanxide™ process, developed by erstwhile Lanxide Corp. (Urquhart 1991). One of the Lanxide processes is called DIMOX™, which stands for directed metal oxidation process. A schematic of the directed metal oxidation process is shown in Fig. 7.4. The first step in this process is to make a preform, which in the case of a particulate composite can be a ceramic green body. In the case of a fibrous composite, filament winding or a fabric lay-up may be used to make a preform. A barrier to stop growth of the matrix material is placed on the preform surfaces. In this method, a molten metal is subjected to directed oxidation, i.e., the desired reaction product forms on the surface of the molten metal and grows outward. The metal is supplied continuously to the reaction front by a wicking action through channels in the oxidation product. For example, molten aluminum in air will get

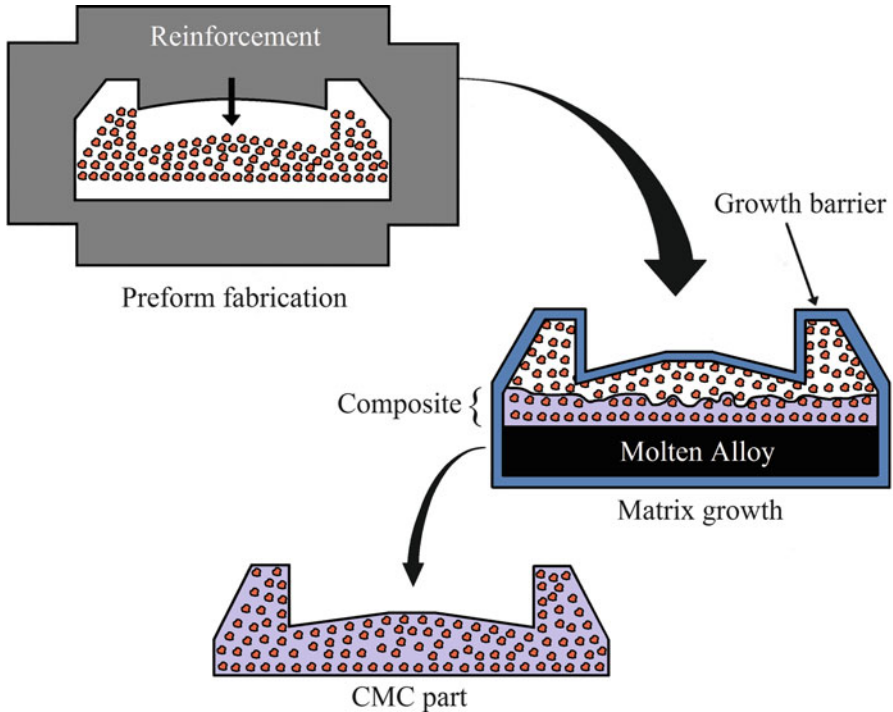
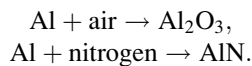


Fig. 7.4 Schematic of the directed metal oxidation process of Lanxide Corp. (Courtesy of Lanxide Corp.)

oxidized to aluminum oxide. If one wants to form aluminum nitride, then molten aluminum is reacted with nitrogen. The reaction can be represented as follows:



The end product in this process is a three-dimensional, interconnected network of a ceramic material plus about 5–30% of unreacted metal. When filler particles are placed next to the molten metal surface, the ceramic network forms around these particles. As we said earlier, a fabric made of a continuous fiber can also be used. The fabric is coated with a proprietary coating to protect the fiber from highly reducing aluminum and to provide a weak interface, which is desirable for enhanced toughness in CMCs. Some aluminum (6–7 wt.%) remains at the end of the process. This must be removed if the composite is to be used at temperatures above the melting point of aluminum (660°C). On the other hand, the presence of a residual metal can be exploited to provide some fracture toughness in these composites.

Proper control of the reaction kinetics is of great importance in this process. The process is potentially a low-cost process because near-net shapes are possible. Also, good mechanical properties (such as strength and toughness) have been reported (Urquhart 1991). Figure 7.5 shows some fiber reinforced ceramic components made

by this process. Figure 7.5a shows some fiber reinforced ceramic composites for applications in high-temperature gas turbine engine components, while Fig. 7.5b shows heat exchanger and radiant burner tubes, flame tubes, and other high-temperature furnace parts made of particle reinforced ceramic composites.

The main disadvantages of the Lanxide processes are as follows:

- It is difficult to control the chemistry and produce an all-ceramic matrix by this method. There is always some residual metal, which is not easy to remove completely.
- It is difficult to envision the use of such techniques for large, complex parts, such as those required, say, for aerospace applications.

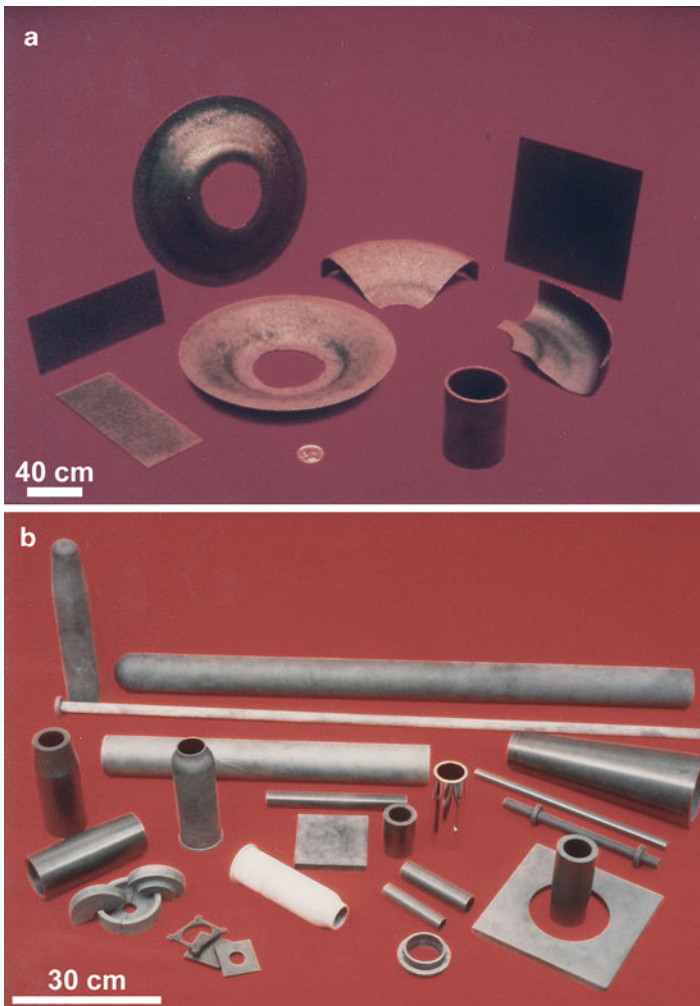
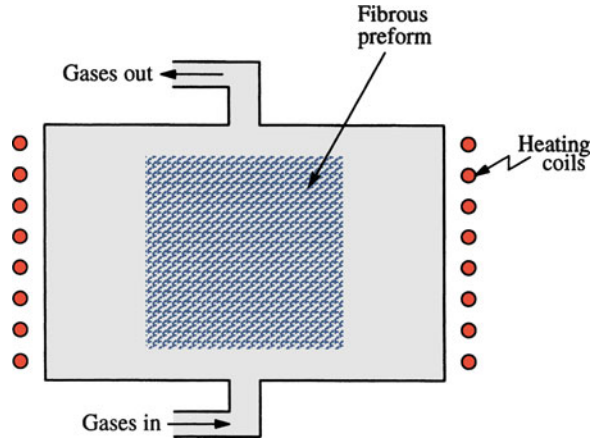


Fig. 7.5 Some fiber reinforced ceramic components made by Dimox process. (a) Fiber reinforced ceramic composites for applications in high-temperature gas turbine engine components. (b) Heat exchanger and radiant burner tubes, flame tubes, and other high-temperature furnace parts made of particle reinforced ceramic composites. (Courtesy of Lanxide Corp.)

Fig. 7.6 Schematic of an isothermal chemical vapor infiltration process



7.1.6 *In Situ Chemical Reaction Techniques*

In situ chemical reaction techniques to produce CMCs are extensions of those used to produce monolithic ceramic bodies. We describe below some of the more important techniques, viz., chemical vapor deposition (CVD) and chemical vapor infiltration (CVI) and different types of reaction bonding techniques.

7.1.6.1 Chemical Vapor Deposition and Chemical Vapor Impregnation

When the chemical vapor deposition (CVD) technique is used to impregnate rather large amounts of matrix material in fibrous preforms, it is called *chemical vapor impregnation* (CVI). Common ceramic matrix materials used are SiC, Si₃N₄, and HfC. The CVI method has been used successfully by several researchers to impregnate fibrous preforms (Fitzer and Hegen 1979; Fitzer and Schlichting 1980; Fitzer and Gadow 1986; Stinton et al. 1986; Burkland et al. 1988). The preforms can consist of yarns, woven fabrics, or three-dimensional shapes.

In very simple terms, in the CVI process a solid material is deposited from gaseous reactants onto a heated substrate. A typical CVD or CVI process would require a reactor with the following parts:

1. A vapor feed system.
2. A CVD reactor in which the substrate is heated and gaseous reactants are fed.
3. An effluent system where exhaust gases are handled.

The chemistry for making ceramic fibers by CVD was given in Chap. 2. The basic chemistry to make a bulk ceramic matrix in and around fibers in a preform remains the same. One can synthesize a variety of ceramic matrixes such as oxides, glasses, ceramics, and intermetallics by CVD. Commonly, the process involves an isothermal decomposition of a chemical compound in the vapor form to yield the

desired ceramic matrix on and in between the fibers in a preform. Figure 7.6 shows a schematic of such an isothermal process. For example, methyltrichlorosilane (CH_3SiCl_3), the starting material to obtain SiC, is decomposed at a temperature between 1,200 and 1,400 K:

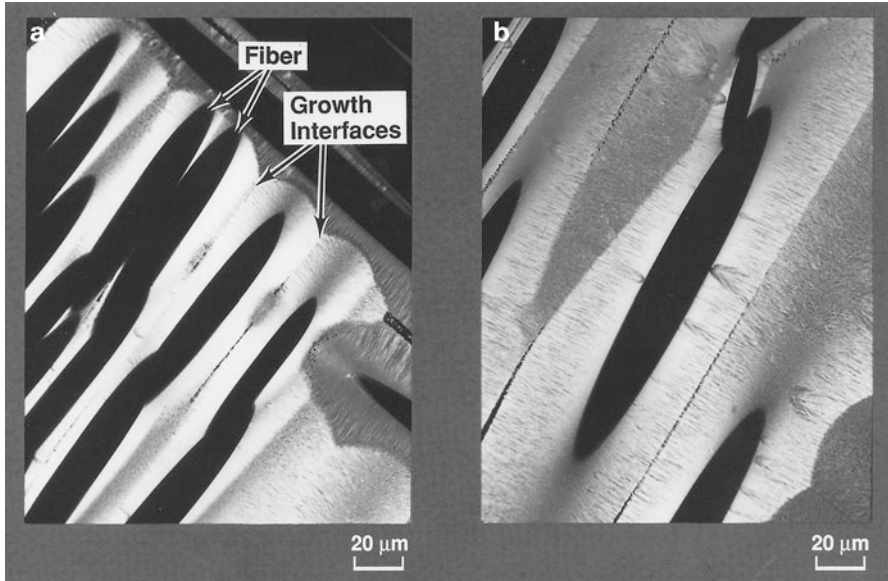


Fig. 7.7 An example of the microstructure of a Nicalon fiber/SiC matrix composite obtained by CVI. (Courtesy of R.H. Jones). Note the growth interfaces within the matrix indicated by *arrows*

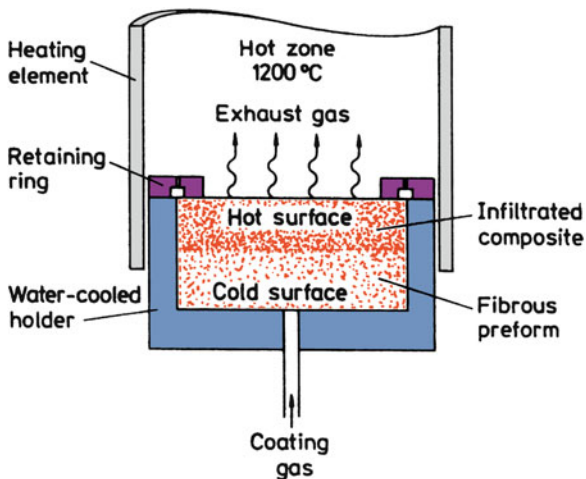


Fig. 7.8 Schematic of a chemical vapor infiltration process with pressure and temperature gradients [after Stinton et al. (1986)]

The vapors of SiC deposit as solid phase on and in between the fibers in a free-standing preform to make the matrix. An example of the microstructure of a SiC/SiC composite obtained by CVI is shown in Figure 7.7. The CVI process is very slow because it involves diffusion of the reactant species to the fibrous substrate, followed by outflow of the gaseous reactant products. The CVI process of making a ceramic matrix is, indeed, a kind of low-stress and low-temperature CVD process, and thus avoids some of the problems associated with high-temperature ceramic processing. However, when the CVI process is carried out isothermally, near surface pores tend to close first, restricting the gas flow to the interior of the preform. This necessitates multiple cycles of impregnation, surface machining, and reinfiltration to obtain an adequate density. One can avoid some of these problems to some extent by using a forced gas flow and a temperature gradient. A schematic of one version of this process is shown in Fig. 7.8 (Stinton et al. 1986). A graphite holder in contact with a water-cooled metallic gas distributor holds the fibrous preform. The bottom and side surfaces thus stay cool while the top of the fibrous preform is exposed to the hot zone, creating a steep thermal gradient. The reactant gaseous mixture passes unreacted through the fibrous preform because of the low temperature. When these gases reach the hot zone, they decompose and deposit on and between the fibers to form the matrix. As the matrix material gets deposited in the hot portion of the preform, the preform density and thermal conductivity increase and the hot zone moves progressively from the top of the preform toward the bottom. When the composite is formed completely at the top and is no longer permeable, the gases flow radially through the preform, exiting from the vented retaining ring.

This variant of CVI, which combines forced gas flow and temperature gradient, avoids some of the problems mentioned earlier. Under these modified conditions, 70–90% dense SiC and Si₃N₄ matrices can be impregnated in SiC and Si₃N₄ fibrous preforms in less than a day. Under conditions of plain CVI, it would take several weeks to achieve such densities, i.e., one can reduce the processing time from several days to less than 24 h. One can also avoid using binders in this process with their attendant problems of incomplete removal. The use of a graphite holder simplifies the fabrication of the preform, and the application of a moderate pressure to the preform can result in a higher-than-normal fiber volume fraction in the final product. The final obtainable density in a ceramic body is limited by the fact that closed porosity starts at about 93–94% of theoretical density. It is difficult to impregnate past this point.

Advantages of a CVI technique or any variant thereof include:

- Good mechanical properties at high temperatures.
- Large, complex shapes can be produced in a near-net shape.
- Considerable flexibility in the fibers and matrices that can be employed (oxide and nonoxide).

Among the disadvantages, one should mention that the process is slow and expensive.

7.1.6.2 Reactive Consolidation or Liquid-Phase Sintering

Siliconized silicon carbide is the name given to a composite of SiC grains in a silicon matrix. Molten silicon reacts with carbon fibers to form SiC. The original geometry of the carbon fibers is retained. Carbon fiber in the form of cloth, tow, felt, or mat is used as a precursor. A preform is made of carbon fiber and infiltrated with liquid silicon. Silicon reacts with carbon fibers to form SiC fibers in a Si matrix. Typical composition of the resultant composite is Si (30–50%) + SiC fiber. The silicon matrix limits the use temperature to about 1,400°C. A big advantage of SiC/Si composites is that the constituents are in chemical equilibrium and they have closely matched thermal expansion coefficients.

In another version of this process, a liquid phase forms as a result of an exothermic reaction between elemental powders. A good example is that from the field of intermetallics, e.g., nickel aluminides. The following steps are involved:

1. Mix nickel and aluminum in stoichiometric proportions.
2. Cold isostatic press to 70% theoretical density to obtain a green body.
3. Vacuum encapsulate the green body in a 304 stainless steel can.
4. Subject the canned material to reactive hot isostatic pressing.

7.1.7 Sol–Gel

Sol–gel techniques, which have been used to make conventional ceramic materials, can also be used to make ceramic matrix materials in the interstices of a fibrous preform. We described the sol–gel technique in Chap. 2. To recapitulate, a solution containing metal compounds, e.g., a metal alkoxide, acetate, or halide, is reacted to form a sol. The sol is converted to a gel, which in turn is subjected to controlled heating to produce the desired end product: a glass, a glass–ceramic, or a ceramic. Characteristically, the gel-to-ceramic conversion temperature is much lower than that required in a conventional melting or sintering process. Some of the advantages of these techniques for making composites are the same as the ones for monolithic ceramics, viz., lower processing temperatures, greater compositional homogeneity in single-phase matrices, and potential for producing unique multiphase matrix materials, etc. Specifically, in regard to composite material fabrication, the sol–gel technique allows processing via liquids of low viscosity such as the ones derived from alkoxides. Among the disadvantages of sol–gel are high shrinkage and low yield compared to slurry techniques. The fiber network provides a very high surface area to the matrix gel. Consequently, the shrinkage during the drying step, frequently, results in a large density of cracks in the matrix. Generally, repeated impregnations are required to produce a substantially dense matrix.

It is easy to see that many of the polymer handling and processing techniques can be used for sol–gel as well. Impregnation of fibrous preforms in vacuum and filament winding are two important techniques. In filament winding, fiber tows or

rovings are passed through a tank containing the sol, and the impregnated tow is wound on a mandrel to a desired shape and thickness. The sol is converted to gel and the structure is removed from the mandrel. A final heat treatment then converts the gel to a ceramic or glass matrix.

The sol–gel technique can also be used to prepare prepreps by the slurry infiltration method. The sol in the slurry acts as a binder and coats fibers and glass particles. The binder burnout step is thus eliminated because the binder, being of the same composition as the matrix, becomes part of the glass matrix. An advantage of this sol–gel-based slurry method is that consolidation can be done at lower temperatures. Among the problems, one should mention that the coating layer on the fiber is porous, frequently carbon-rich, and nonuniform.

7.1.8 Polymer Infiltration and Pyrolysis

Just as polymeric precursors can be used to make ceramic fibers (see Chap. 2), we can use polymeric precursors to form a ceramic matrix in a composite. This technique is called polymer infiltration and pyrolysis (PIP). It is an attractive processing route because of its relatively low cost, small amounts of residual porosity and minimal degradation of the fibers. Moreover, this approach allows near net-shape molding and fabrication technology that is able to produce nearly fully dense composites. In PIP, the fibers are infiltrated with an organic polymer, which is heated to fairly high temperatures and pyrolyzed to form a ceramic matrix. Due to the relatively low yield of polymer to ceramic, multiple infiltrations are used to densify the composite.

Polymeric precursors for ceramic matrices allow one to use conventional polymer composite fabrication technology that is readily available, and take advantage of processes used to make polymer matrix composites (French 1996; Hurwitz et al. 1989). These include complex shape forming and fabrication. Furthermore, by processing and pyrolyzing at lower temperatures (compared to sintering and hot-pressing, for example) one can avoid fiber degradation and the formation of unwanted reaction products at the fiber/matrix interface.

Among the desirable characteristics of a preceramic polymer are (more of wish list):

- High ceramic yield from polymer precursor.
- Precursor that yields a ceramic with low free carbon content (which will oxidize at high temperatures).
- Controllable molecular weight, which allows for solvent solubility and control over viscosity for fabrication purposes.
- Low temperature crosslinking of the polymer, which allows resin to harden and maintain its dimensions during the pyrolysis process.
- Low cost and toxicity.

Most preceramic polymer precursors are formed from chloroorganosilicon compounds to form poly(silanes), poly(carbosilanes), poly(silazanes), poly(borosilanes), poly(silsesquioxanes), and poly(carbosiloxanes). The synthesis reaction involves the dechlorination of the chlorinated silane monomers. Since a lot of the chlorosilane monomers are formed as byproducts in the silicone industry, they are inexpensive and readily available. The monomers can be further controlled by an appropriate amount of branching which controls important properties such as the viscosity of the precursor as well as the amount of ceramic yield. All silicon based polymer precursors lead to an amorphous ceramic matrix, where silicon atoms are tetrahedrally arranged with nonsilicon atoms. This arrangement is similar to that found in amorphous silica. High temperature treatments typically lead to crystallization and slight densification of the matrix, which results in shrinkage. At high temperatures, the amorphous ceramic begins to form small domains of crystalline phase, which are more thermodynamically stable. Si–C matrices derived from polycarbosilane begin to crystallize at 1,100–1,200°C, while Si–C–O (polysiloxanes) and Si–N–C (polysilazanes) remain amorphous to 1,300–1,400°C.

Typically the range of the molecular weight of the polymer is tailored, followed by shaping of the product. The polymer is then crosslinked and finally pyrolyzed in an inert or reactive atmosphere (e.g., NH_3) at temperatures between 1,000 and 1,400°C. The pyrolysis step can be further subdivided into three steps. In the first step, between 550 and 880°C, an amorphous hydrogenated compound of the type Si ($\text{C}_a\text{O}_b\text{N}_c\text{B}_d$) is formed. The second step involves nucleation of crystalline precipitates such as SiC, Si_3N_4 , and SiO_2 at temperatures between 1,200 and 1,600°C. Grain coarsening may also result from consumption of any residual amorphous phase and reduction of the amount of oxygen due to vaporization of SiO and CO. Porosity is typically on the order of 5–20 vol.% with pore sizes of the order of 1–50 nm. It should be noted that the average pore size and volume fraction of pores decrease with increasing pyrolysis temperature, since the amount of densification (and shrinkage) becomes irreversible at temperatures above the maximum pyrolysis temperature

Among the disadvantages of PIP, we can list:

- Low yield accompanies the polymer-to-ceramic transformation.
- Large shrinkage, which typically causes cracking in the matrix during fabrication. Due to shrinkage and weight loss during pyrolysis, residual porosity after a single impregnation is on the order of 20–30%.
- To reduce the amount of residual porosity, multiple impregnations are needed. Reimpregnation is typically conducted with a very low viscosity prepolymer so that the slurry may wet and infiltrate the small micropores that exist in the preform. Usually, reimpregnation is done by immersing the part in the liquid polymer in a vacuum bag, while higher viscosity polymers require pressure impregnation. Typically, the amount of porosity will reduce from 35% to less than 10% after about five impregnations.

Significant gas evolution also occurs during pyrolysis (French 1996). Thus, it is advisable to allow these volatile gases to slowly diffuse out of the matrix, especially for thicker parts. Typically, pyrolysis cycles ramp to somewhere between 800 and 1,400°C over periods of 1–2 days, to avoid delamination. Recall that pyrolysis must be done at a temperature below the crystallization temperature of the matrix (or large volume changes will occur) and below the degradation temperature of the reinforcing fibers. The pyrolysis atmosphere is most commonly argon or nitrogen, although in ammonia, we obtain a pure amorphous silicon nitride with low amounts of free carbon. Fitzer and Gadov (1986) used repeated infiltration and in situ thermal decomposition of porous reaction-bonded ceramics to process $\text{Si}_3\text{N}_4/\text{SiC}$ composites. The following steps are taken in processing the composites:

- (i) Prepare a porous SiC or Si_3N_4 fibrous preform with some binder phase.
- (ii) Fibrous preform is evacuated in an autoclave.
- (iii) Samples are infiltrated with molten precursors, silazanes or polycarbosilanes, at high temperature (780 K) and the argon or nitrogen pressure is slowly increased from 2 to 40 MPa. The high temperature results in a transformation of the oligomer silane to polycarbosilane and simultaneous polymerization at high pressures.
- (iv) Infiltrated samples are cooled and treated with solvents.
- (v) Samples are placed in an autoclave and the organosilicon polymer matrix is thermally decomposed in an inert atmosphere at a high pressure and at temperature in the 800–1,300 K range.
- (vi) Steps (ii) through (v) are repeated to attain an adequate density. To produce an optimum matrix crystal structure, the material is annealed in the 1,300–1,800 K range.

Polymer-derived ceramic matrix composites, similar to carbon/carbon composites (see Chap. 8), typically have a cracked matrix from processing as well as a number of small pores. The large amount of shrinkage and cracking in the matrix can be contained, to some extent, by the additions of particulate fillers to the matrix, which, when added to the polymer reduce shrinkage and stiffen the matrix material in the composite. Figure 7.9 shows schematically the role of fillers in reducing the porosity and cracking in the final product. Particulate or whisker ceramics used as fillers in the polymeric matrix can serve a variety of purposes:

- Reduce and disrupt the formation of matrix cracks that form during shrinkage of the polymer.
- Enhance ceramic yield by forming reaction products during pyrolysis.
- Strengthen and toughen the weak amorphous matrix and increase the interlaminar shear strength of the composite.

The filler must be submicrometer in size in order to penetrate the tow bundle and the filler's coefficient of thermal expansion must match that of the polymeric matrix. The filler must not be used in very high fractions and the slurry should not be forced into the reinforcing fibers since abrasion of the fiber fabric may take place. This is especially true with hard, angular fillers or ceramic whiskers.

Typically, the volume fraction of filler is 15–25% of the matrix volume fraction. High filler loading may result in an increase in interply spacing and lower volume fraction of fibers.

When an “active” filler phase is added to the polymer, the following generic reaction can take place to form new carbide phase (Greil 1995):



where P is the polymer, T is the active filler, C is the ceramic, and G is the gaseous by-product, and M is the carbide phase formed. By controlling the amount of filler, the degree of shrinkage can be controlled.

Fiber architecture may have an impact in regard to polymer infiltration and pyrolysis (PIP). One of the key factors is wetting of the fiber bundles. During pyrolysis, the precursor shrinks around the fibers, so cracks are introduced. For example, two dimensional woven fabrics seem to have less propensity in developing interlaminar cracks than do cross-ply or unidirectional architectures. Satin weaves are preferred over plain weaves because more uniform cracking is achieved and large cracks between weave crossover points are avoided (Hurwitz 1992). Due to the looser nature of the satin weave (it is more drapeable), better wetting and densification may take place, although the loose nature of the weave also makes it more difficult to handle.

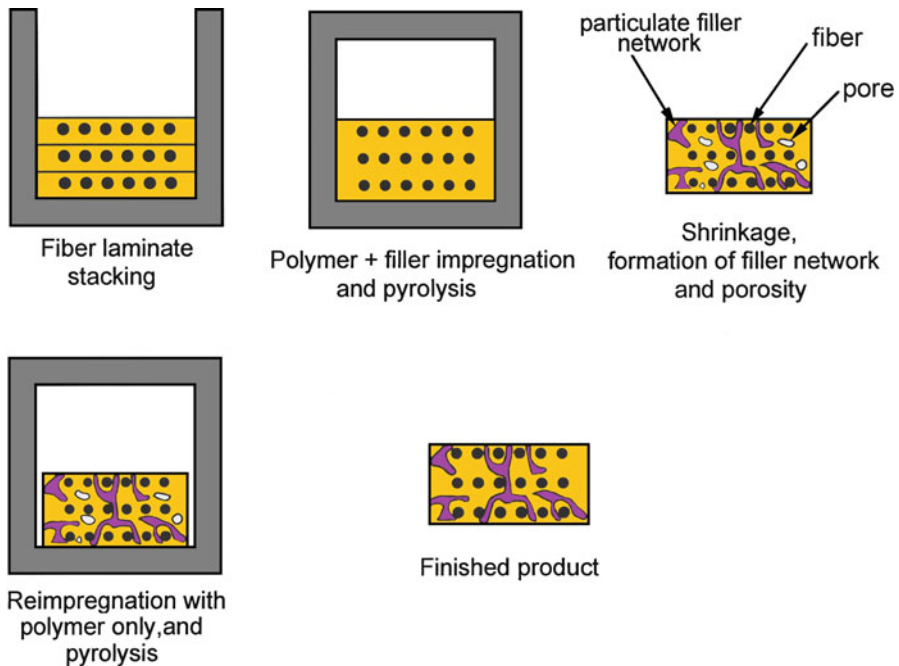


Fig. 7.9 The role of fillers in reducing the porosity and cracking in the final CMC product

7.1.9 Electrophoretic Deposition

The phenomenon of electrophoresis has been known since the beginning of the nineteenth century, but its applications in processing of ceramics and ceramic composites are relatively recent. Electrophoretic deposition (EPD) should not be confused with electroplating. In electroplating, ions are the moving species and they undergo ion reduction on deposition. In EPD, on the other hand, solid particles migrate with no charge reduction on deposition. Also, the deposition rate in EPD is ≈ 1 mm/min while in electroplating it ≈ 0.1 $\mu\text{m}/\text{min}$. Electrophoretic deposition is a relatively simple and inexpensive technique, which can be profitably exploited for infiltration of tightly woven preforms made of fibers (Illston et al. 1993). EPD makes use of nanoscale ceramic particles in a stable nonagglomerated form (such as in a sol or colloidal suspension) and exploits their net surface electrostatic charge characteristics while in suspension. On application of an electric field such surface charge carrying particles will migrate toward and deposit on an electrode. If the deposition electrode is replaced by a conducting fibrous preform, the suspended particles will be attracted into and deposited within it, providing an appropriate means of effectively infiltrating densely packed fibrous bundles. A schematic of the basic EPD cell is shown in Fig. 7.10a while an example of the microstructure of Nextel 720 fiber reinforced mullite matrix composite is shown in Fig. 7.10b. The movement of ceramic sol particles in an aqueous suspension within an electric field is governed by the field strength, and the pH, ionic strength and viscosity of the solution (Illston et al. 1993). The electrophoretic mobility of charged particles in a suspension is given by the following equation called the Smoluchowski equation:

$$\text{electrophoretic mobility} = \frac{U}{E} = \frac{\varepsilon\zeta}{4\pi\eta},$$

where U is the velocity, E is the field strength, ε is the dielectric constant, ζ is the zeta potential, and η is the viscosity. The zeta potential is a parameter that characterizes a suspension. It can be determined by measuring particle velocity in an electric field. According to the above equation, a suitable suspension for EPD should have the following characteristics: a high particle surface charge, a high dielectric constant of the liquid phase, and a low viscosity. In addition, a low conductivity of the suspending medium to minimize solvent transport would be desirable (Kaya et al. 2000, 2009).

7.1.10 Self-Propagating High-Temperature Synthesis

The self-propagating high-temperature synthesis (SHS) technique involves synthesis of compounds without an external source of energy. One exploits exothermic reactions to synthesize ceramic compounds, which are difficult to fabricate by

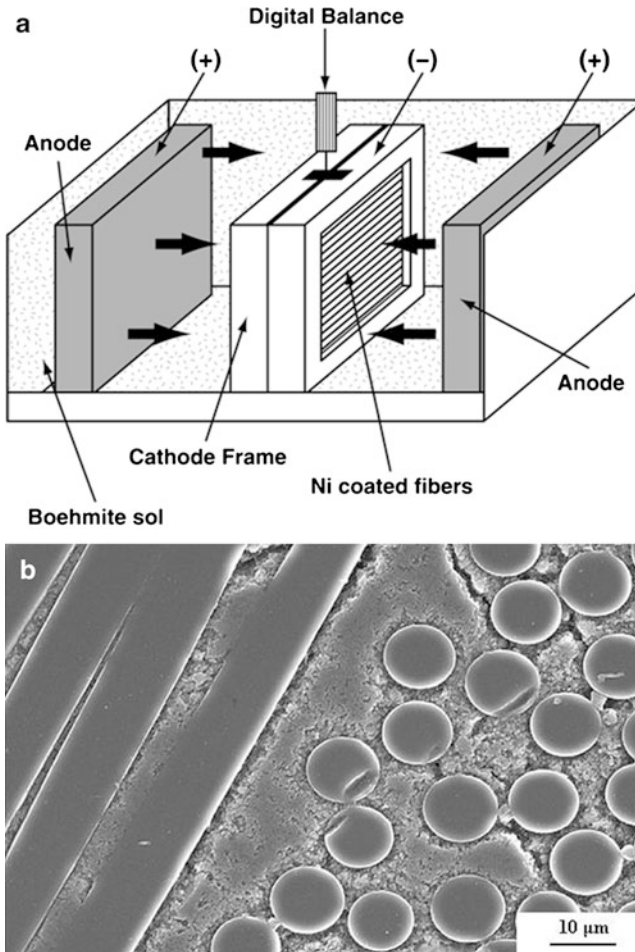


Fig. 7.10 (a) Schematic of the basic electrophoretic deposition (EPD) cell. (b) Microstructure of Nicalon 720 fiber/mullite composite made by electrophoretic deposition (from Kaya et al. 2009)

conventional techniques. For example, one can mix titanium powder and carbon black, cold press the mixture, and ignite the compact at the top in a cold-walled vessel. A combustion wave will pass through the compact, giving titanium carbide.

Among the salient features of SHS are:

- High combustion temperature (up to 4,000°C).
- Simple, low-cost equipment.
- Good control of chemical composition.
- Different shapes and forms can be obtained.

This technique can be used to produce a variety of refractory materials. The main disadvantage is that SHS products are very porous, because of the fairly large

porosity in the original mix of reactants and because of the large volume change that results when the reactants transform to the products. Any adsorbed gases at the elevated temperatures used during this process can also add to the porosity of the final product. Synthesis concomitant with densification can improve the situation to some extent. This involves application of high pressure during the combustion or immediately after the completion of the combustion reaction, when the product temperature is still quite high. Hot pressing, rolling, and shock waves are some of the techniques used to apply the necessary pressure.

Many ceramics, such as borides, carbides, nitrides, silicides, and sialons, and composites, such as $\text{SiC}_w + \text{Al}_2\text{O}_3$, have been synthesized by means of SHS. The SHS process gives a weakly bonded compact. Therefore, the process is generally followed by breaking the compact, milling, and consolidation by some technique such as HIPing. Explosive or dynamic compaction can result in a relatively dense product. A good example of an SHS process to make composites is the XDTM process, wherein exothermic reactions are used to produce multiphase alloy powders. These are hot pressed at $\sim 1,450^\circ\text{C}$ to full density. Reinforcement in the form of particles, whiskers, and platelets can be added to the master alloy to make a composite. A good example is that of TiB_2 particles, about $1\ \mu\text{m}$ in diameter, distributed in intermetallic matrices such as TiAl , $\text{TiAl} + \text{Ti}_3\text{Al}$, and NiAl .

7.2 Interface in CMCs

In general, for CMCs one must satisfy the following compatibility requirements: thermal expansion compatibility and chemical compatibility. Ceramics have a limited ductility, and in the fabrication of CMCs one uses high temperatures. Thus, thermal mismatch on cooling from high temperatures can cause cracking in matrix (or fiber). Thermal strain in composites is proportional to $\Delta\alpha\Delta T$, where $\Delta\alpha = \alpha_f - \alpha_m$, α_f and α_m being the linear expansion coefficients of the fiber and matrix, respectively, and ΔT is the temperature interval. There is, of course, another complication, namely, fiber expansion coefficients are also sometimes not equal in the axial and radial directions. Carbon fiber in particular has the following axial and radial coefficients:

$$\begin{aligned}\alpha_a &\approx 0, \\ \alpha_r &\approx 8 \times 10^{-6} \text{ K}^{-1}.\end{aligned}$$

If $\Delta\alpha$ is positive, i.e., $\alpha_f > \alpha_m$, the matrix is compressed on cooling, which is beneficial because it leads to an increase in the tensile stress at which matrix cracking will occur. Conversely, if $\Delta\alpha$ is negative, i.e., $\alpha_f < \alpha_m$, the matrix experiences tension, which, if ΔT is sufficiently large, can cause matrix cracking. In the radial direction, if $\Delta\alpha$ is positive, the fibers tend to shrink away from the matrix on cooling, which results in a reduced interfacial bond strength. If, however, $\Delta\alpha$ is negative, the fiber matrix bond strength can even be improved.

Table 7.1 A comparison of damage resulting from the thermal expansion mismatch in some carbon fiber reinforced systems^a

Matrix	α_m^b ($10^{-6} \text{ }^\circ\text{C}^{-1}$)	T_c^c ($^\circ\text{C}$)	E (GPa)	σ_{mu}^d (MPa)	ϕ_a^e	ϕ_r^e	Damage
MgO	13.6	1,200	300	200	25	10	Severe cracking
Al ₂ O ₃ (80 % dense)	8.3	1,400	230	300	9	0.3	Severe cracking
Soda-lime glass	8.9	480	60	100	2.6	0.3	Localized cracks
Borosilicate glass	3.5	520	60	100	1.1	-1.4	Uncracked
Glass-ceramic	1.5	1,000	100	100	1.5	-6.5	Uncracked

^aType I carbon fibers $\alpha_a \approx 0$, $\alpha_r \approx 8 \times 10^{-6} \text{ K}^{-1}$

^b α_m is the matrix thermal expansion coefficient

^c T_c is the temperature below which little stress relaxation can occur

^d σ_{mu} is the matrix strength.

^e ϕ_a and ϕ_r are the thermal expansion mismatch parameters

Source: Adapted with permission from Phillips (1983)

Matrix cracking resulting from thermal mismatch is, comparatively speaking, a more serious problem in short fiber composites than in continuous fiber composites. The reason is that in a ceramic matrix containing aligned continuous fibers, transverse microcracks appear in the matrix, but fibers continue to hold the various matrix blocks together and the composite can still display a reasonable amount of strength. In a randomly oriented short fiber composite, owing to increased stress at the fiber ends, matrix cracking occurs in all directions and the composite is very weak. We can define a thermal expansion mismatch parameter for axial and radial directions in an aligned fiber composite as (Sambell et al. 1972):

$$\phi_a, \phi_r = \Delta\alpha\Delta T(E_m/\sigma_m).$$

Table 7.1 makes a comparison of damage resulting from thermal expansion mismatch in some carbon fiber reinforced ceramic matrix composites. Note that only glass and glass-ceramic matrices (low modulus materials) show no damage.

Chemical compatibility between the ceramic matrix and the fiber involves the same thermodynamic and kinetic considerations as with other composite types. Quite frequently, the bond between fiber and ceramic matrix is simple mechanical interlocking. During fabrication (by hot pressing) or during subsequent heat treatments, the fiber/matrix bond could be affected by the high temperatures attained because of any chemical reaction between the fiber and matrix or because of any phase changes in either one of the components. Sambell et al. (1972) studied the zirconia reinforced magnesia composite system in which there occurs a chemical reaction at 1,600°C. At temperatures less than 1,600°C, the composites showed a weak fiber/matrix interface and fiber pullout occurred during mechanical polishing. Upon heat treating at 1,600°C, however, because of the interfacial reaction and the resultant improved bonding, no damage was observed upon mechanical polishing. Heat treatment at 1,700°C resulted in the complete destruction of the zirconia fibers and the distribution of zirconia to grain boundaries in magnesia. Thus, as we noted in the case of MMCs (Chap. 6), it is important to be

able to control the interfacial bond by means of controlled chemical reactions between components. Chokshi and Porter (1985), working with SiC/Al₂O₃ system, observed a reaction layer on the fiber surface after creep testing in air. Auger electron microscopy analysis showed a mullite layer with large glassy phase regions along grain boundaries. The following interfacial reaction was proposed:



and reaction kinetics were modeled by an equation of the form

$$x^2 \approx Dt,$$

where x is the reaction zone thickness, $D = D_0 \exp(-Q/kT)$, Q is the activation energy, k is Boltzmann's constant, T is the temperature in kelvin, and t is the time in seconds.

The nature of the bond between fiber and ceramic matrix is thought to be predominantly mechanical. In carbon fiber reinforced glass or glass-ceramics there is little or no chemical bonding (Davidge 1979; Phillips et al. 1972; Prewo 1982). Evidence for this is the low transverse strength of these composites and the fact that one does not see matrix material adhering to the fibers on the fracture surface. The bond is thought to be entirely mechanical with the ceramic matrix penetrating the irregularities present on the carbon surface. Shear strength data on carbon fiber in borosilicate glass and lithium-aluminosilicate glass-ceramics (LAS) show that the borosilicate glass composites have double the shear strength of LAS composites. The reason for this is the different radial shrinkage of fibers from the matrix during cooling. Calculated radial contractions of fiber from the matrix are 2.4×10^{-8} m for the LAS ceramic and 0.9×10^{-8} m for the glass-ceramic composite (Phillips 1983). Shrinkage reduces the mechanical interlocking and thus the fiber/matrix bond.

In ceramic matrix composites, interfacial roughness-induced radial stress becomes quite important because it affects the interface debonding, the sliding friction of debonded fibers, and the fiber pullout length. Fiber pullout is one of the important energy dissipating fracture processes in fiber reinforced ceramic or glass matrix composites. An absence of strong chemical bond and a purely mechanical bond at the fiber/matrix interface is highly desirable for the fiber pullout to occur. In regard to the mechanical bonding, a number of researchers have pointed out the importance of interfacial roughness in ceramic matrix composites (CMCs) (Jero 1990; Jero and Kerans 1990; Carter et al. 1991; Jero et al. 1991; Kerans and Parthasarathy 1991; Mackin et al. 1992; Mumm and Faber 1992; Venkatesh and Chawla 1992; Chawla et al. 1993a, b; Sorensen 1993). If an interfacial coating is used, its coefficient of expansion must also be taken into account. As shown by Chawla and coworkers (Venkatesh and Chawla 1992; Chawla et al. 1993a, b), even when the coefficients of thermal expansion of the coating, fiber, and matrix are such that a radial tensile stress exists at the fiber/coating interface after cooling from an elevated processing temperature, fiber pullout may not occur because of a strong mechanical bonding due to a

roughness-induced clamping at the fiber/matrix. Thus, a tensile thermal stress in the radial at the interface is desirable factor. A radial tensile stress at the interface will encourage fiber debonding and slippage, which in turn result in high toughness and high work of fracture. We can express the interfacial sliding resistance in terms of interfacial shear stress as (Hutchinson and Jensen 1990):

$$\begin{aligned}\tau &= \tau_o - \mu\sigma_n, & (\sigma_n < 0), \\ \tau &= \tau_o, & (\sigma_n \geq 0),\end{aligned}$$

where σ_n is the stress normal to the interface, μ is the coefficient of friction, and τ_o is the sliding resistance when σ_n is positive (tensile). Kerans and Parthasarathy (1991) included interface surface roughness in a detailed treatment of fiber debonding and sliding during both pushout and pullout experiments. They modeled the effect of fiber surface roughness as an increase in the interfacial strain mismatch, leading to an increase in the interfacial normal pressure.

The effective normal stress σ_n at the interface is the algebraic sum of the two radial components: residual thermal stress and roughness-induced stress. We can write

$$\sigma_n = \sigma_t + \sigma_r,$$

where σ_t and σ_r are thermal and roughness-induced stresses, respectively.

The thermal stress and roughness-induced stress can be expressed as

$$\begin{aligned}\sigma_t &= \beta(\Delta\alpha\Delta T), \\ \sigma_r &= \beta(A/r),\end{aligned}$$

where $\Delta\alpha$ is the difference in thermal expansion coefficients between matrix and fiber, ΔT is the temperature differential ($T_2 - T_1$), β is a term containing elastic constants, A is the amplitude of roughness, and r is the fiber radius.

7.3 Properties of CMCs

An important feature of CMCs is matrix microcracking, which does not have a parallel in MMCs or PMCs. As mentioned earlier, the relative elastic modulus values of fiber, E_f and matrix, E_m are very important in CMCs. The ratio E_f/E_m determines the extent of matrix microcracking. Typically, the strain-to-fracture value of a ceramic matrix is very low. Thus, in MMCs and in thermoplastic PMCs, the matrix failure strain (ϵ_m) is considerably greater than that of fibers. Most unreinforced metals show, a strain-to-fracture $\epsilon_m > 10\%$ while most polymers fail between 3 and 5% strain. Thus, in both MMCs and PMCs fiber failure strain controls the composite failure strain. Typically, fibers such as boron, carbon, and silicon carbide show failure strain values of $\sim 1-2\%$. Compare this with the failure strains of less than 0.05% for most ceramic matrix materials. The situation in regard

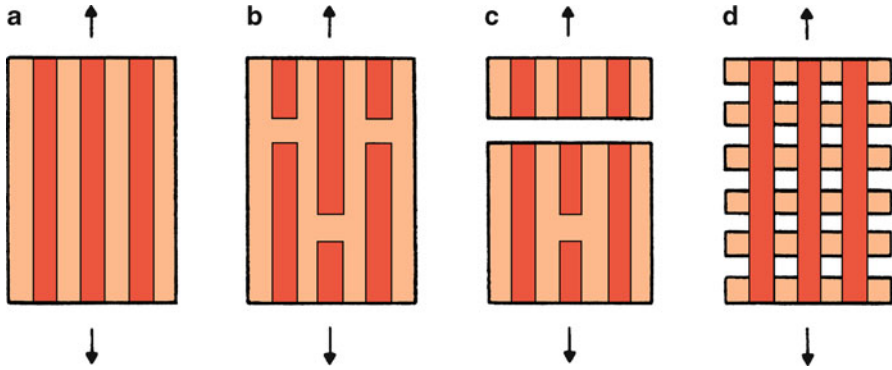


Fig. 7.11 (a) Original crack-free situation. (b) In the case of MMCs and PMCs, fibers fail first at various weak points distributed along their lengths. The composite will fail along a section that has the maximum number of fiber fractures. (c) In a strongly bonded CMC, fiber and matrix would fail simultaneously at matrix failure strain. (d) In a weakly bonded CMC, however, the matrix will start cracking first and the fibers will be bridging the matrix blocks

to fiber and/or matrix failure is shown in a simplified manner in Fig. 7.11. The crack-free original situation is shown in Fig. 7.11a. In the case of MMCs and PMCs, fibers fail first at various weak points distributed along their lengths; see Fig. 7.11b. The final failure of the composite will occur along a section that has the most fiber fractures. In a strongly bonded CMC, fiber and matrix would fail simultaneously at matrix failure strain and a situation similar to that shown in Fig. 7.11c will prevail. In a weakly bonded CMC, however, the matrix will start cracking first and the fibers will be bridging the matrix blocks, Fig. 7.11d shows an idealized situation. Thus, from a toughness point of view, in general, we do not want too strong a bond in a CMC because it would make a crack run through the specimen. A weak interface, however, would lead to fiber-bridging of matrix microcracks.

A CMC with even a microcracked ceramic matrix can retain some reasonable strength ($\sigma_c \simeq \sigma_f V_f$) and there are applications, such as bushings, where such a damage-tolerant characteristic would be very valuable because in the absence of fibers bridging the cracks, the monolithic matrix would simply disintegrate. The disadvantage, of course, is that matrix microcracking provides an easy path for environmental attack of the fibers and the fiber/matrix interface. Let us consider an idealized situation of a fiber reinforced, unidirectionally aligned, CMC, loaded in the longitudinal direction. Assume that the CMC has proper interface, i.e., it is damage-tolerant. At a stress σ_0 , the stress–strain curve will show a dip, indicating the incidence of periodic matrix cracking, see Fig. 7.12. Because the fibers have enough strength to support the load in the presence of a damaged matrix (a very desirable feature indeed), the stress–strain curve will continue to rise until, at a stress marked σ_u , the fiber bundle fails. At this point, the phenomenon of fiber pullout starts. The extent of this fiber pullout region depends critically on the interfacial frictional resistance. The fiber/matrix interface has a lot to do with the form of the stress–strain curve. If the bonding is too strong, matrix cracking will be accompanied by a small amount of fiber pullout, which is an undesirable characteristic from the toughness

viewpoint, as we shall see in Sect. 7.4. Increased stiffness and strength were observed in a unidirectionally aligned composite consisting of continuous carbon fibers (50% V_f) in a glass matrix compared to the unreinforced glass matrix (Davidge 1979). But more importantly, a large increase in the work of fracture occurred. The increased work of fracture is a result of the controlled fracture behavior of the composite, while the unreinforced matrix failed in a catastrophic manner.

Fiber length, or more precisely, the fiber aspect ratio (length/diameter), fiber orientation, relative strengths and moduli of fiber and matrix, thermal expansion mismatch, matrix porosity, and fiber flaws are the important variables that control the performance of CMCs. Sambell et al. (1974) showed that, for ceramic matrix materials containing short, randomly distributed carbon fibers, a weakening effect occurred rather than a strengthening effect. This was attributed to the stress concentration effect at the extremities of randomly distributed short fibers and thermal expansion mismatch. Aligned continuous fibers do lead to a real fiber reinforcement effect. The stress concentration at fiber ends is minimized and higher fiber volume fractions can be obtained. At very high fiber volume fractions, however, it becomes difficult to eliminate the porosity in the ceramic matrix. Figure 7.12 shows that the strength increases in a linear fashion for carbon fiber/glass matrix composites, for up to $\sim 55\% V_f$ (Phillips et al. 1972). Beyond $55\% V_f$, the high matrix porosity led to a drop in the strength. The Young's modulus also increased linear with V_f , as shown in Fig. 7.13; at higher V_f it deviated from linearity owing to matrix porosity and possible fiber misalignment (Phillips et al. 1972).

Creep resistance of a ceramic such as alumina can be improved by adding fibers or whiskers. Silicon carbide SiC whisker reinforced alumina showed superior creep-resistance than polycrystalline alumina (Chokshi and Porter 1985); see Figure 7.14. This figure shows, on a log-log plot, the creep strain rate as a function of stress at a constant temperature. Note that the composite has a higher-stress exponent than the unreinforced matrix. The higher-stress exponent indicates a change in the operating creep mechanism. The exponent for polycrystalline alumina is about 2, and this is rationalized in terms of some kind of diffusion creep being the controlling mechanism. A stress exponent of about 5, which was observed for the composite, is indicative of a dislocation creep mechanism being in operation. Observation of the specimens deformed in creep in transmission electron microscope showed dislocation activity.

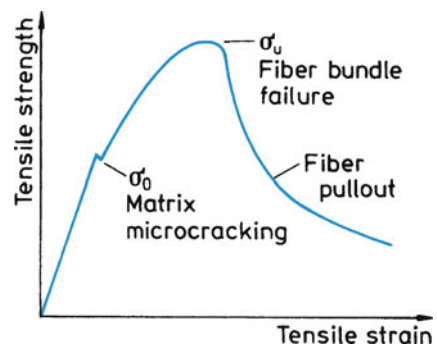


Fig. 7.12 Stress-strain curve of an aligned CMC in the longitudinal direction showing a damage-tolerant behavior

Fig. 7.13 Linear increase in strength with fiber volume fraction V_f up to ~55 % in carbon fiber/glass matrix composites [after Phillips et al. (1972), used with permission]

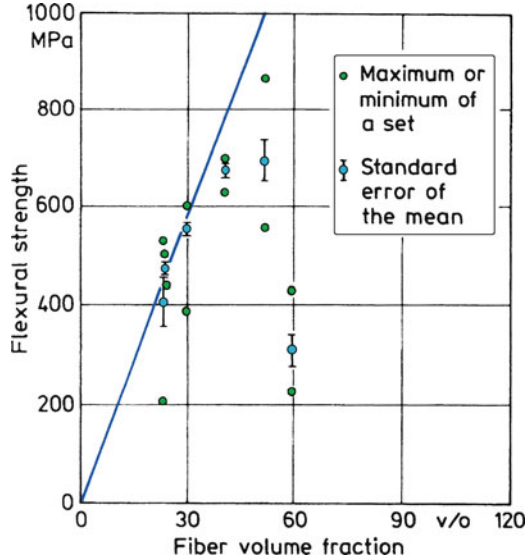
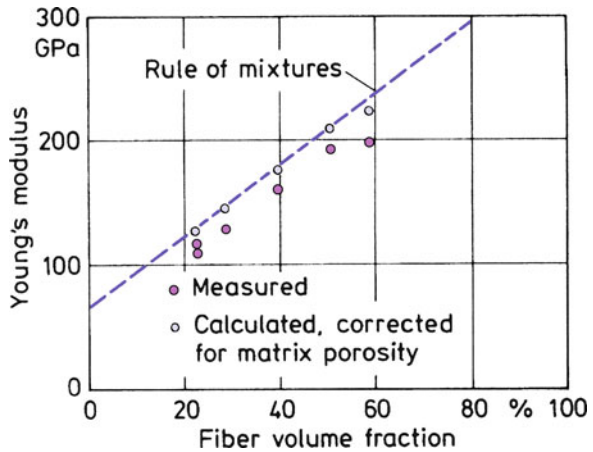


Fig. 7.14 Linear increase in Young’s modulus with fiber volume fraction, V_f . At higher V_f , it deviates from linear owing to matrix porosity and possible fiber misalignment [Phillips et al. (1972)]



7.4 Toughness of CMCs

Many concepts have been proposed for augmenting the toughness of ceramic matrix materials (see Chawla 2003, for a summary). Table 7.2 lists some of these concepts and gives the basic requirements for the models to be valid. Clearly, more than one toughness mechanism may be in operation at a given time. Matrix microcracking, fiber/matrix debonding leading to crack deflection and fiber pullout, and phase transformation toughening are all basically energy-dissipating processes that can result in an increase in toughness or work of fracture. Figure 7.16 shows schematically some of these toughness mechanisms or energy-dissipating mechanisms that can be brought to play in CMCs.

Fig. 7.15 Plots of creep strain rate as function of stress at constant temperature for silicon carbide whisker reinforced alumina and unreinforced alumina. SiC_w/Al₂O₃ is more creep-resistant than unreinforced polycrystalline alumina (Chokshi and Porter 1985). Note that the composite has a higher stress exponent than the unreinforced matrix

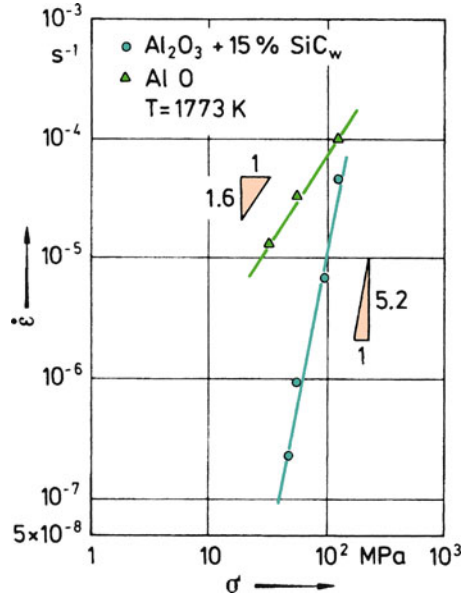


Table 7.2 Ceramic matrix composite toughening mechanisms

Mechanism	Requirement
1. Compressive prestressing of the matrix	$\alpha_f > \alpha_m$ will result in an axial compressive prestressing of the matrix after fabrication.
2. Crack impeding	Fracture toughness of the second phase (fibers or particles) is greater than that of the matrix locally. Crack is either arrested or bows out (line tension effect).
3. Fiber (or whisker) pullout	Fibers or whiskers having high transverse fracture toughness will cause failure along fiber/matrix interface leading to fiber pullout on further straining.
4. Crack deflection	Weak fiber/matrix interfaces deflect the propagating crack away from the principal direction.
5. Phase transformation toughening	The crack tip stress field in the matrix can cause the second-phase particles (fibers) at the crack tip to undergo a phase transformation causing expansion ($\Delta V > 0$). The volume expansion can squeeze the crack shut.

Work on carbon and SiC fiber reinforced glass and glass–ceramic composites (Brennan and Prewo 1982; Prewo et al. 1986; Fitzer and Hegen 1979; Prewo 1982) has shown that tough and strong CMCs could be made if extensive fiber pullout and a controlled fracture behavior of the CMC (i.e., a damage-tolerant fracture behavior) could be brought to play. Let us examine a Nicalon fiber/glass–ceramic composite. A scanning electron micrograph of a hot-pressed Ba–Si–Al–O–N glass–ceramic containing Nicalon fibers composite is shown in Fig. 7.17. (Herron and Risbud 1986). Note the crystalline nature of the matrix. The fracture surface of

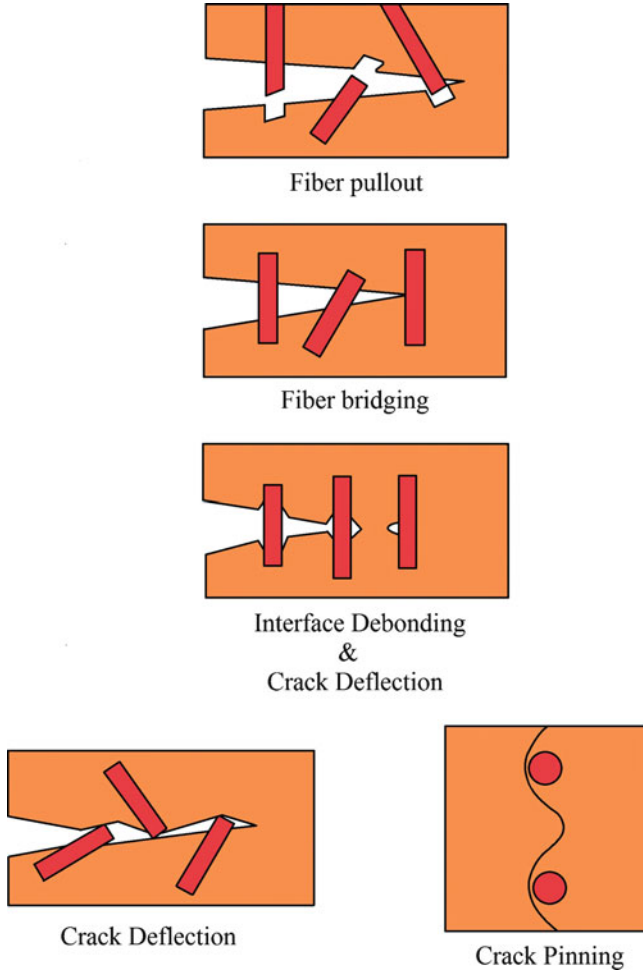


Fig. 7.16 Schematic of some toughness or energy-dissipating mechanisms that can be brought to play in CMCs

this composite (Fig. 7.18) showed the phenomenon of fiber pullout, indicating a weak fiber/matrix bond. The fibers were bonded to the matrix by an amorphous layer whose characteristics changed with heat treatment; a carbon-rich layer was also observed on the fiber surface (Herron and Risbud 1986). Remnants of the interfacial amorphous layer adhering to the Nicalon fibers can be seen in Fig. 7.18. One can accentuate the propensity of fiber pullout by applying a suitable coating on the fiber, which would control the interfacial characteristics. This was observed in the composite system Nicalon/pyrolytic carbon coating/SiC, as shown in Fig. 7.19 wherein we see Nicalon fibers pulled out of the matrix (Chawla et al. 1994). Among oxide ceramic matrix materials, alumina and mullite are quite important. In particular, SiC whisker reinforced alumina composites (20–30% by volume of SiC

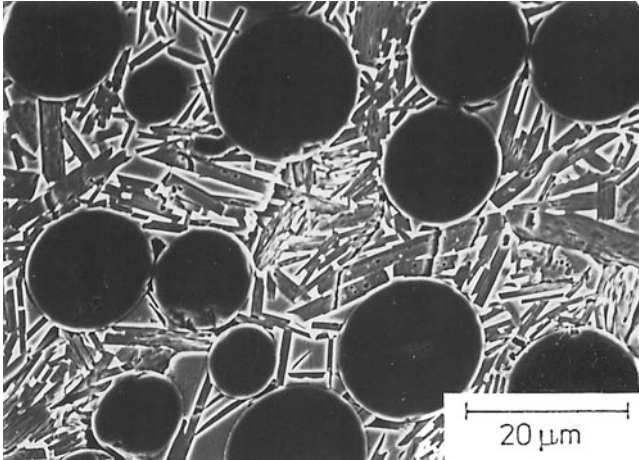


Fig. 7.17 Scanning electron micrograph of a hot-pressed Nicalon fiber/Ba-Si-Al-O-N glass-ceramic matrix composite [from Herron and Risbud (1986), used with permission]

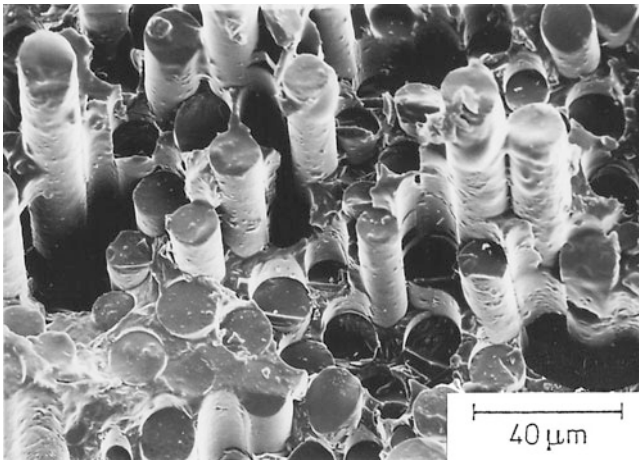


Fig. 7.18 Fracture surface of Nicalon/Ba-Si-Al-O-N glass-ceramic matrix composite showing fiber pullout [Herron and Risbud (1986), used with permission]

whiskers in alumina, made by hot pressing) showed impressive gains in toughness and strength (Becher and Wei 1984; Wei and Becher 1984; Tiegs and Becher 1986); see Figs. 7.20 and 7.21. A typical fine-grained monolithic alumina has toughness (K_{Ic}) of 4–5 MPa m^{1/2} and flexural strength between 350 and 450 MPa. Al₂O₃ containing 20% by volume of SiC whiskers showed a K_{Ic} of 8–8.5 MPa m^{1/2} and a flexural strength of 650 MPa; these levels were maintained up to about 1,000°C.

Fig. 7.19 Fiber pullout in a Nicalon/pyrolytic carbon coating/SiC matrix composite. Some broken fibers can be seen inside the cylindrical cavities left by the pulled out fibers (courtesy of N. Chawla)

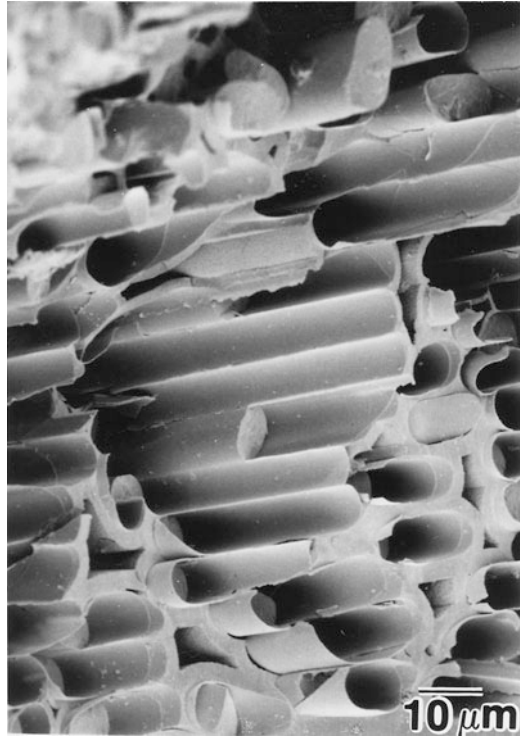


Fig. 7.20 High-temperature strength increases as a function of the SiC whiskers volume fraction in SiC_w/Al₂O₃ [from Tiegs and Becher (1986), used with permission]

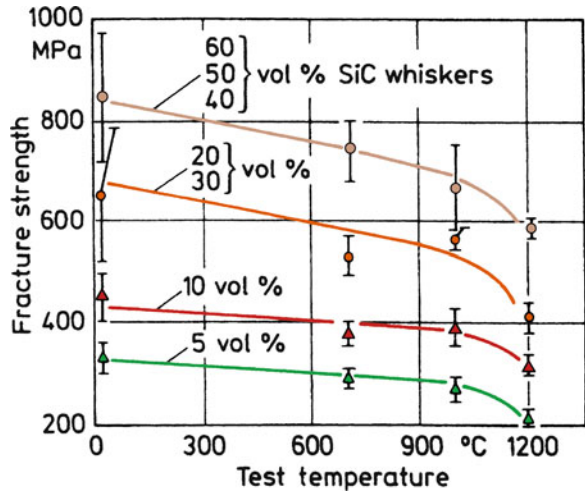
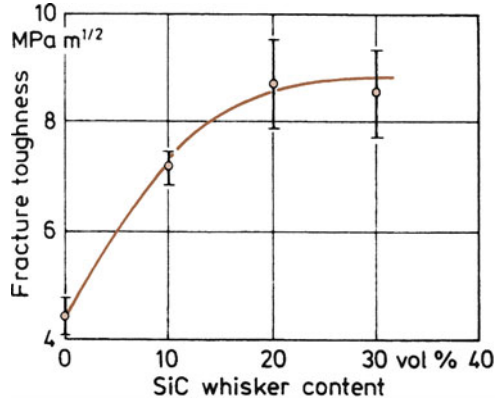


Fig. 7.21 Toughness gains are obtained by incorporating SiC whiskers in alumina [Tiegs and Becher (1986), used with permission]



It is worth reemphasizing that the main goal in CMCs is to increase the toughness; modulus and strength are already high in most ceramics. If the crack growth in a ceramic can be impeded by some means, then a higher stress would be required to make it move. Fibers (metallic or ceramic) can play the role of toughening agents in ceramic matrices. Metallic fiber reinforced ceramics will clearly be restricted to lower temperatures than ceramic fiber reinforced ceramic matrices. As described above, glass and glass–ceramic matrices containing carbon fibers (Phillips et al. 1972; Davidge 1979; Prewo and Brennan 1980; Prewo 1982; Brennan and Prewo 1982; Prewo et al. 1986) have been shown to have fiber pullout as the dominant toughening mechanism. Basically, fiber pullout requires that the strength transferred to the fiber during the ceramic matrix fracture be less than the fiber ultimate strength, σ_{fu} , and that an interfacial shear stress be developed that is greater than the fiber/matrix interfacial strength, τ_i ; that is the interface must fail in shear. For a given fiber of radius r , we have the axial tensile stress in the fiber given by (we derive this expression in Chap. 10)

$$\sigma_f = 2\tau_i \left(\frac{l_c}{r} \right),$$

where l_c is the critical fiber length and $\sigma_f < \sigma_{fu}$. The tensile stress increases from a minimum at both fiber ends and attains a maximum along the central portion of the fiber (see Fig. 10.13). Fibers that bridge the fracture plane and whose ends terminate within $l_c/2$ from the fracture plane will undergo pullout, while those with ends further away will fracture when $\sigma_f = \sigma_{fu}$. A crack deflection mechanism also requires that as a matrix crack reaches the interface, it gets deflected along the interface rather than passing straight through the fiber. Consider a fiber reinforced ceramic that has mechanical bonding at the interface, i.e., frictional gripping of the fiber by the matrix. When we load this composite, a crack initiates in the matrix and starts propagating in the matrix normal to the interface. If the fiber/matrix interface is weak, then interfacial shear and lateral contraction of fiber and matrix will result in fiber/matrix debonding and crack deflection away from its principal direction

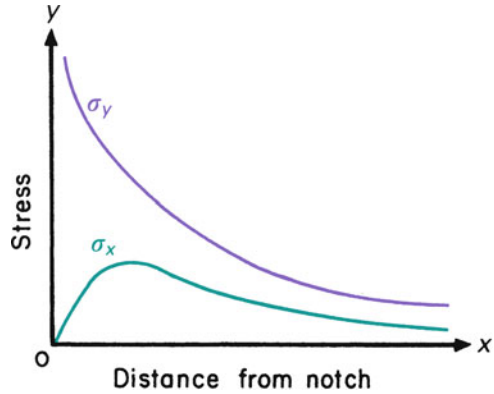
(normal to the interface). A further increment of crack extension in the principal direction will occur after some delay. On continuing stressing of the composite, the fiber/matrix interface delamination continues and fiber failure will occur at some weak point along its length. This is followed by broken fiber ends being pulled out against the frictional resistance of the interface and finally causing a total separation. We discuss this process in terms of crack deflection criteria further in this section.

Let us summarize the requirements for strong and tough CMCs. Avoiding processing-related flaws in the matrix and in the fiber would appear to be an elementary and straightforward recommendation. If processing results in large flaws in the matrix, the composite fracture strain will be low. In this respect, fiber bridging of cracks in a CMC will result in a reduced flaw size in the matrix. This, in turn, will help achieve higher applied strains before crack propagation in the matrix than in an unreinforced, monolithic ceramic (Aveston et al. 1971). A weak interfacial bond, as pointed out earlier, leads to crack deflection at the fiber/matrix interface and/or fiber pullout. Use of a high-volume fraction of continuous fibers stiffer than the matrix will give increased stiffness, which results in a higher stress level being needed to produce matrix microcracking and a higher composite ultimate tensile stress, as well as a high creep resistance (DiCarlo 1985). A high-volume fraction and a small fiber diameter also provide a sufficient number of fibers for crack bridging and postponing crack propagation to higher strain levels. A small-diameter fiber also translates into a small l_c , the critical length for effective load transfer from matrix to fiber (see Chap. 10). Although a weak interface is desirable from a toughness point of view, it provides a short circuit for environmental attack. An ability to maintain a high strength level and high inertness at high temperatures and in aggressive atmospheres is highly desirable.

An interesting technique to obtain enhanced toughness in CMCs involves coatings that undergo phase transformation involving volume change. Kriven and colleagues (Kriven 1995; Zhu and Kriven 1996; Kriven and Lee 1998) have exploited interfacial coatings with compositions that have multiple polymorphs wherein transformations can be triggered by shear stress. Under the action of shear stress at the tip of an oncoming crack, a transformation is induced in the coating, causing a volume or shape at the fiber/matrix interface. Energy from the crack is then dissipated by the following means:

1. Dissipation of crack energy through nucleation of transformation
2. Possible autocatalytic nucleation of transformation along the interface promoting interfacial debonding and fiber pullout
3. Increased surface energy contribution from interfacial microcracking or shearing from the transformation
4. Increased frictional work that the crack must do to achieve interfacial debonding, i.e., optimal results will require control of coating thickness

Fig. 7.22 Stress distribution at a crack tip. The stress is applied along the y -axis and the crack is propagating along the x -axis [after Cook and Gordon (1964)]



7.4.1 Crack Deflection at the Interface in a CMC

The phenomenon of crack deflection at the fiber/matrix has been analyzed by many researchers. Cook and Gordon (1964) analyzed the phenomenon of crack deflection or the formation of secondary cracks at a weak interface in terms of the state of stress at the crack tip. Let us consider a crack advancing in the matrix in a direction perpendicular to the fiber/matrix interface. Cook and Gordon estimated the strength of the interface necessary to cause a diversion of the crack from its original direction when both fiber and matrix have the same elastic constant. At the tip of any crack, a triaxial state of stress (plane strain) or a biaxial stress (plane stress) is present. Figure 7.22 shows schematically the stress distribution at a crack tip. The main applied stress component, σ_y , has a very high value at the crack tip, and decreases sharply with distance from the crack tip. The stress component acting normal to the interface, σ_x , is zero at the crack tip; it rises to a maximum value at a small distance from the crack tip and then falls off in a manner similar to σ_y . It is easy to visualize that if the tensile strength of the fiber/matrix interface is less than the maximum value of σ_x , then the interface will fail in front of the crack tip. According to the estimates of Cook and Gordon, an interfacial strength of 1/5 or less than that of the main stress component, σ_y , will cause the opening of the interface in front of the crack tip.

More sophisticated analyses of crack interaction with an interface, based on the fracture energy considerations, have been proposed (He and Hutchinson 1989; Evans and Marshall 1989; Rühle and Evans 1988; Gupta 1991; Gupta et al. 1993). He and Hutchinson's results give the conditions for fiber/matrix debonding in terms of the fracture of the interface and that of the fiber; see Fig. 7.23. We obtain a plot of G_i/G_f vs. α , where G_i is the mixed-mode interfacial fracture energy of the interface, G_f is the mode I fracture energy of the fiber, and α is a measure of elastic anisotropy. The parameter α is defined as

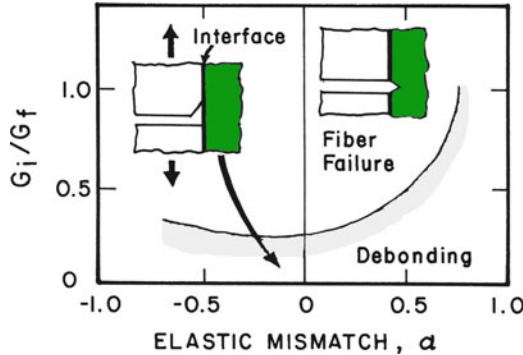


Fig. 7.23 Fiber/matrix debonding criterion in terms of the energy requirements. G_i is the mixed-mode interfacial fracture energy of the interface, G_f is the mode I fracture energy of the fiber, and α is a measure of elastic anisotropy, $\bar{E} = (E/1 - \nu^2)$ [after He and Hutchinson (1989)]

$$\alpha = \frac{\bar{E}_1 - \bar{E}_2}{\bar{E}_1 + \bar{E}_2},$$

where

$$\bar{E} = \frac{E}{1 - \nu^2},$$

where E is the Young’s modulus and ν is the Poisson’s ratio and the subscripts 1 and 2 refer to the matrix and fiber, respectively. The plot in Fig. 7.23 shows the conditions under which the crack will deflect along the interface or propagate through the interface into the fiber. For all values of G_i/G_f below the curve, interface debonding is predicted. In area above the curve, the crack will penetrate through the interface into the fiber. Consider the special case of zero elastic mismatch, i.e., for $\alpha = 0$. In this case, the fiber/matrix interface will debond for G_i/G_f less than about 0.25. Conversely, for G_i/G_f greater than 0.25, the crack will propagate across the interface into fiber. In general, for the elastic mismatch, α greater than zero, the minimum interfacial toughness, G_i , required for interface debonding increases, i.e., high modulus fiber tends to favor debonding. One shortcoming of this analysis is that it treats both the fiber and matrix as isotropic materials. This is not always true, especially for the fiber. Also, in practice, it is difficult to obtain the values of quantities such as the interfacial fracture energy. Gupta et al. (1993) have derived strength and energy criteria for crack deflection at a fiber/matrix interface for several composite systems, taking due account of the anisotropic nature of the fiber. Their experimental technique, laser spallation experiment using a laser Doppler displacement interferometer, was described in Chap. 4. By this technique they could measure the tensile strength of a planar interface. They have tabulated the required values of the interface strength and fracture toughness for delamination in number of ceramic, metal, intermetallic, and polymer matrix composites.

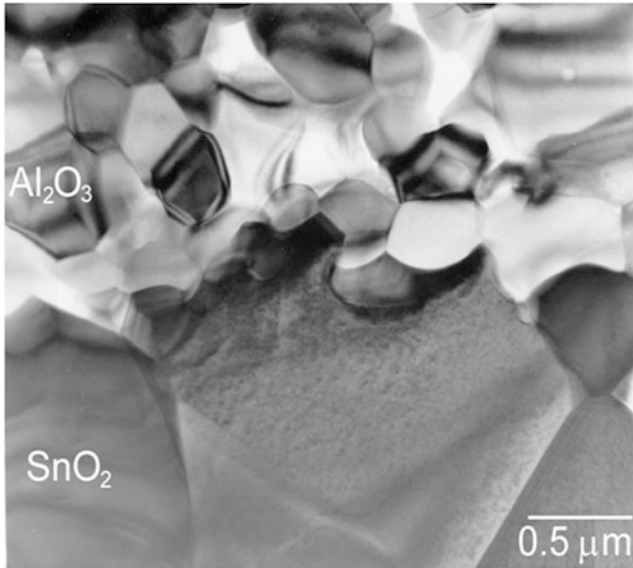


Fig. 7.24 Roughness induced mechanical keying at the interface between alumina and SnO₂. Note the tortuous nature of the interface. TEM [Gladysz et al. (1999)]

We end this section by describing a simple and practical way of analyzing the crack deflection problem at the interface in a CMC. This involves evaluation of the state of stress at the interface. In Sect. 7.2, we discussed the state of stress at the fiber/matrix interface by taking into account the thermal stresses induced by processing and interfacial roughness induced stresses. Considering the overall stress state at the interface, one can modify the roughness induced radial stress by choosing a fiber with a smooth surface or by applying a smooth coating on the fiber (Chawla et al. 2000). A rough interface results in strong mechanical keying, which can prevent interfacial debonding and fiber pullout. A smooth interface, on the other hand, leads to weak keying, which is desirable for crack deflection and fiber pullout. For example, one can use coatings that bond weakly with alumina (e.g., SnO₂, LaPO₄), fugitive coatings, layered oxides (mica type) with easy cleavage planes, etc. It is important that there should not be any chemical reaction between the coating and fiber or matrix. Also, thermal mismatch between should result, in the as-fabricated state, a residual tensile stress at the interface in the radial direction. Figure 7.24 brings home the idea of roughness induced mechanical keying at the interface. It shows a TEM micrograph of the interface region between alumina fiber and SnO₂ coating (Gladysz et al. 1999). Note the tortuous nature of the interface. Such a high degree of roughness will result in a partial fiber pullout, even when the thermal stress state is favorable. Figure 7.25 shows this for an alumina fiber/glass matrix composite (Venkatesh and Chawla 1992). Note the rough surface of the alumina fiber due to its small grain size. The situation changes dramatically, if we choose an alumina fiber with a smooth surface. This is shown in Fig. 7.26 where the fiber is single crystal alumina, which has no grain

Fig. 7.25 Fracture surface of alumina fiber/ SnO_2 coating–glass matrix composite showing partial fiber pullout. Note the rough surface of the alumina fiber due to its small grain size



Fig. 7.26 Fracture surface single crystal alumina fiber/ SnO_2 /glass composite showing fiber pullout. This fiber is single crystal alumina, which has no grain boundaries and is, therefore, very smooth. Crack deflection at the interface leads to fiber pullout



boundaries and is, therefore, very smooth (Venkatesh and Chawla 1992). Crack deflection at the interface leads to fiber pullout etc., which contribute to toughness (see also Chap. 10). For detailed analysis of this important topic of interface engineering for toughness, the reader is referred to a review by Chawla et al. (2000).

7.5 Thermal Shock Resistance

Thermal shock resistance is a very important characteristic for ceramics and ceramic composites that are meant to be used at high temperatures and must undergo thermal cycling. We define a thermal shock resistance (TSR) parameter as

$$\text{Thermal shock resistance} = \frac{\sigma k}{E\alpha},$$

where σ is the fracture strength, k is the thermal conductivity, E is the Young's modulus, and α is the coefficient of thermal expansion. Most ceramics have low thermal conductivity which is one problem. But high a coefficient of thermal expansion, α , will aggravate the situation further. Thus, common soda-lime glass and alumina have a high α , about $9 \times 10^{-6} \text{ K}^{-1}$. This makes them very poor in TSR. If we reduce CaO and Na₂O in the common glass, and add B₂O₃ to form a borosilicate, we get a special glass that has an $\alpha = 3 \times 10^{-6} \text{ K}^{-1}$. Such a glass will show superior TSR and is commercially available under the trade names, Pyrex or Duran glass. Glass-ceramics such as lithium aluminosilicates (LAS) have an α close to zero and thus excellent TSR. LAS are used to make the Corningware which can be taken directly from the freezer to the cooking range or oven without causing it to shatter!

Boccaccini et al. (1997a, b) studied the cyclic thermal shock behavior of Nicalon fiber reinforced Duran glass matrix composites. The thermal mismatch between the fiber and the matrix in this system is almost zero. A decrease in Young's modulus and a simultaneous increase in internal friction as a function of thermal cycles were observed. The magnitude of internal friction was more sensitive to microstructural damage than Young's modulus. An interesting finding of theirs involved the phenomenon of crack healing when the glass matrix composite was cycled above the glass transition temperature of the matrix. We discuss this topic further in Chap. 13.

7.6 Applications of CMCs

Ceramic matrix composites find applications in many areas. A convenient classification of the applications of CMCs is aerospace and nonaerospace. Materials-related drivers for applications of CMCs in the aerospace field are:

- High specific stiffness and strength leading to a weight reduction, and, consequently, decreased fuel consumption.
- Reduction in fabrication and maintenance cost.
- Higher operating temperatures leading to a greater thermal efficiency.
- Longer service life.
- Signature reduction, which is valuable in stealth technology (reduce the distance at which a vehicle can be detected).

CMCs can lead to improvements in aerospace vehicles including aircraft, helicopters, missiles, and reentry vehicles. Projected skin temperatures in future hypersonic aircraft are higher than 1,600°C. Other parts, such as radomes, nose tips, leading edges, and control surfaces, will experience only slightly lower temperatures. Currently, one uses sacrificial, nonload-bearing thermal-protection materials on load-bearing components.

Next we give a description of some nonaerospace applications of CMCs.

7.6.1 Cutting Tool Inserts

An important area of CMC applications is that of cutting tool inserts. Silicon carbide whisker reinforced alumina ($\text{SiC}_w/\text{Al}_2\text{O}_3$) composites are used as cutting tool inserts for high-speed cutting of superalloys. For example, in the cutting of Inconel 718, $\text{SiC}_w/\text{Al}_2\text{O}_3$ composite tools show performance that is three times better than conventional ceramic tools, and eight times better than cemented carbides. Among the characteristics that make CMCs good candidates for cutting tool inserts are the following:

- Abrasion resistance
- Thermal shock resistance
- Strength
- Fracture toughness
- Thermal conductivity

Commonly, the volume fraction of SiC_w is 30–45%, and they are made by hot pressing. Figure 7.27 shows the microstructure of such a composite.

7.6.2 Ceramic Composite Filters

Candle-type filters consisting of Nextel™ 312 ceramic fibers in a silicon carbide matrix (see Fig. 7.28) can be used to remove particulate matter from high-temperature gas streams up to 1,000°C. The collected particles are removed by reverse pulse jet cleaning. The high-temperature capability of such filters can eliminate the need to cool the gas stream prior to filtration, which may increase process efficiency and eliminate the cost and complexity of gas dilution, air scrubbers, or heat exchangers. The ceramic

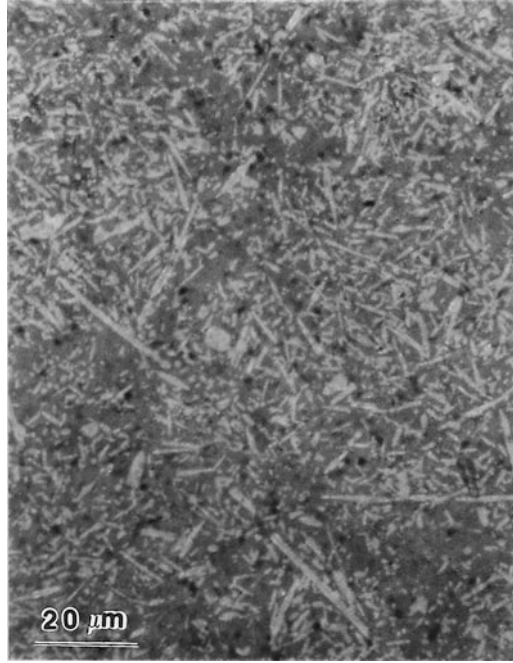


Fig. 7.27 Microstructure of SiC whisker reinforced alumina composite tool insert made by hot pressing



Fig. 7.28 A candle-type filter consisting of Nextel™ 312 ceramic fibers in a silicon carbide matrix. The filter is 1.3 m long. Such filters are used to remove particulate matter from high-temperature gas streams up to 1,000 °C (courtesy of 3M Co.)

fibers toughen the composite construction and result in a filter with excellent resistance to thermal shock and catastrophic failure. The light weight (900 g) of such a filter reduces the strength requirements of the tube sheet, and the excellent thermal shock resistance provides protection. The 3M ceramic composite filter is designed for advanced coal-fired power-generation systems, such as pressurized fluidized bed combustion (PFBC), and integrated gasification combined cycle (IGCC). Among its features are the following:

- High-temperature capability
- Resistance to thermal shock
- Lightweight
- Resistance to catastrophic failure

Potential applications of such filters include:

- Pressurized fluidized bed combustion (PFBC)
- Integrated gasification combined cycle (IGCC)
- Incineration

Supports made of Nicalon fiber reinforced glass matrix composites are used as pad inserts and takeout paddles in direct hot glass-contact equipment (Beier and Markmann 1997).

7.6.3 *Other Applications of CMCs*

Potentially, CMCs can find applications in heat engines, components requiring resistance to aggressive environments, special electronic/electrical applications, energy conversion, and military systems (Schioler and Stiglich 1986).

An interesting application is a radiant burner tube made of CMCs. Heat transfer between two objects can occur by conduction when the two objects are in contact, by convection such as by mixing of hot and cold fluids, or by radiation which involves transmission of electromagnetic waves through space (even vacuum). In a radiant burner tube, heat is transferred from combustion gases to the radiant tube and then by radiation that energy is transferred to the load (the material to be heated). Radiant tube burners are useful in situations where combustion products must not come in contact with the material to be heated, i.e., they are an indirect heating burning meaning the heat is transferred without any direct flame or combustion exhaust. Radiant tube burner systems are designed to reduce nitrous oxide in the burning process. This radiant heat transfer from the tube to the object to be heated is proportional to the fourth power of the temperature. Thus, a ceramic radiant burner tube that can be operated at a higher temperature than say a metallic alloy tube will be more efficient. The problem is that monolithic ceramics lack adequate toughness and thermal shock resistance to be of much use. Hence, the effort to use the radiant tubes made of continuous fiber reinforced ceramic composites that show superior toughness and thermal shock resistance.

Among the barriers that need to be overcome for large-scale applications of CMCs are the high production costs, accepted design philosophy, and the lack of models for strength and toughness. Complicated shapes are difficult to make economically by hot pressing. Sintering or sintering followed by hot isostatic pressing (HIP) are the alternate routes for nonglassy matrices.

References

- Aveston J, Cooper GA, Kelly A (1971) In: The properties of fibre composites. IPC Science & Technology, Guildford, p 15
- Barclay SJ, Fox JR, Bowen HK (1987) *J Mater Sci* 22:4403
- Becher PF, Wei GC (1984) *Commun Am Ceram Soc* 67:259
- Beier W, Markmann S (1997) *Adv Mater Processes* 152:37
- Bhatt RT (1986) NASA TN-88814
- Bhatt RT (1990) *J Mater Sci* 25:3401
- Boccaccini AR, Pearce DH, Janczak J, Beier W, Ponton CB (1997a) *Mater Sci Technol* 13:852
- Boccaccini AR, Ponton CB, Chawla KK (1997b) *Mater Sci Eng A* 241:142
- Bordia RK, Raj R (1988) *J Am Ceram Soc* 71:302
- Brennan JJ, Prewo KM (1982) *J Mater Sci* 17:2371
- Burkland CV, Bustamante WE, Klacka R, Yang J-M (1988) In: Whisker- and fiber-toughened ceramics. ASM Intl, Materials Park, OH, p 225
- Carter WC, Butler EP, Fuller ER Jr (1991) *Scripta Metall Mater* 25:579–584
- Chawla KK (2003) *Ceramic matrix composites*, 2nd edn. Kluwer Acad. Pub, Boston, MA
- Chawla KK, Ferber MK, Xu ZR, Venkatesh R (1993a) *Mater Sci Eng A* 162:35–44
- Chawla KK, Xu ZR, Hlinak A, Chung Y-W (1993b) In: *Advances in ceramic-matrix composites*. Am. Ceram. Soc, Westerville, OH, pp 725–736
- Chawla N, Liaw PK, Lara-Curzio E, Lowden RA, Ferber MK (1994) In: *High performance composites: commonality of phenomena*. The Minerals, Metals & Materials Society, Warrendale, PA, p 291
- Chawla KK, Coffin C, Xu ZR (2000) *Intl Mater Rev* 45:165
- Chokshi AH, Porter JR (1985) *J Am Ceram Soc* 68:c144
- Claussen N, Le T, Wu S (1989) *J Eur Ceram Soc* 5:29
- Claussen N, Wu S, Holtz D (1994) *J Eur Ceram Soc* 14:209
- Cook J, Gordon JE (1964) *Proc R Soc Lond A* 228:508
- Cornie JA, Chiang Y-M, Uhlmann DR, Mortensen A, Collins JM (1986) *Am Ceram Soc Bull* 65:293
- Davidge RW (1979) *Mechanical behavior of ceramics*. Cambridge University Press, Cambridge, p 116
- De Jonghe LC, Rahaman MN, Hseuh CH (1986) *Acta Metall* 39:1467
- DiCarlo JA (1985) *J Met* 37:44
- Evans AG (1985) *Mater Sci Eng* 71:3
- Evans AG, Marshall DB (1989) *Acta Metall* 37:2567
- Fitzer E, Gadow R (1986) *Am Ceram Soc Bull* 65:326
- Fitzer E, Hegen D (1979) *Angew Chem* 91:316
- Fitzer E, Schlichting J (1980) *Z Werkstofftech* 11:330
- French JE (1996) In: *Handbook of continuous fiber ceramic composites*. Amer. Ceramic Soc, Westerville, OH, p 269
- Greil P (1995) *J Am Ceram Soc* 78:835
- Gupta V (1991) *MRS Bull XVI*:4:39
- Gupta V, Yuan J, Martinez D (1993) *J Am Ceram Soc* 76:305

- Gladysz GM, Chawla KK (2001) *Composities A* 32:173
- Gladysz GM, Schmücker M, Chawla KK, Schneider H, Joslin DL, Ferber MK (1999) *Journal of Mater Sci* 34:4351
- He MY, Hutchinson JW (1989) *J Appl Mech* 56:270
- Herron M, Risbud SH (1986) *Am Ceram Soc Bull* 65:342
- Hillig WB (1988) *J Am Ceram Soc* 71:C-96
- Homeny J, Vaughn WL, Ferber MK (1987) *Am Ceram Soc Bull* 67:333
- Hurwitz FI (1992) NASA Tech Memo, 105754
- Hurwitz FI, Gyekenyesi JZ, Conroy PJ (1989) *Ceram Eng Sci Proc* 10:750
- Hutchinson JW, Jensen HM (1990) *Mech Mater* 9:139–163
- Illston TJ, Ponton CB, Marquis PM, Butler EG (1993) Manufacture of doped glasses using electrophoretic deposition. In: Duran P, Fernandez JF (eds) *Third euroceramics*, vol 1. Faenza Editrice Iberica, Madrid, p 419
- Jero PD (1990) *Am Ceram Soc Bull* 69:484
- Jero PD, Kerans RJ (1990) *Scripta Metall* 24:2315–2318
- Jero PD, Kerans RJ, Parthasarathy TA (1991) *J Am Ceram Soc* 74:2793–2801
- Kaya C, Boccaccini AR, Chawla KK (2000) *J Am Ceram Soc* 83:1885
- Kaya C, Kaya F, Butler EG, Boccaccini AR, Chawla KK (2009) *J Eur Ceram Soc* 29:1631
- Kellett B, Lange FF (1989) *J Am Ceram Soc* 67:369
- Kerans RJ, Parthasarathy TA (1991) *J Am Ceram Soc* 74:1585–1596
- Kristofferson A, Warren A, Brandt J, Lundberg R et al (eds) *Proc. Int. Conf. HTCMC-1*. Woodhead Pub., Cambridge, p 151
- Kriven WM (1995) *J Phys (France)* 5:C8–C101
- Kriven WM, Lee SJ (1998) *Ceram Eng Sci Proc* 19:305
- Liu HY, Claussen N, Hoffmann MJ, Petzow G (1991) *J Eur Ceram Soc* 7:41
- Mackin TJ, Warren PD, Evans AG (1992) *Acta Metall Mater* 40:1251–1257
- Mumm DR, Faber KT (1992) *Ceram Eng Sci Proc* 7–8:70–77
- Nourbakhsh S, Liang FL, Margolin H (1990) *Metall Trans A* 21A:213
- Nourbakhsh S, Margolin H (1990) *Metall Trans A* 20A:2159
- Phillips DC (1983a) Fabrication of composites. North-Holland, Amsterdam, p 373
- Phillips DC, Sambell RAJ, Bowen DH (1972) *J Mater Sci* 7:1454
- Prewo KM (1982) *J Mater Sci* 17:3549
- Prewo KM (1986) Tailoring multiphase and composite ceramics, vol 20, *Materials science research*. Plenum, New York, p 529
- Prewo KM, Brennan JJ (1980) *J Mater Sci* 15:463
- Prewo KM, Brennan JJ, Layden GK (1986) *Am Ceram Soc Bull* 65:305
- Rahaman MN, De Jonghe LC (1987) *J Am Ceram Soc* 70:C-348
- Raj R, Bordia RK (1989) *Acta Metall* 32:1003
- Ruhle M, Evans AG (1988) *Mater Sci Eng A* 107:187
- Sacks MD, Lee HW, Rojas OE (1987) *J Am Ceram Soc* 70:C-348
- Sambell RAJ, Bowen DH, Phillips DC (1972) *J Mater Sci* 7:773
- Sambell RAJ, Phillips DC, Bowen DH (1974) *Carbon fibres: their place in modern technology*. The Plastics Institute, London, p 16/9
- Schioler LJ, Stiglich JJ (1986) *Am Ceram Soc Bull* 65:289
- Schneider H, Komarneni S (2005) *Mullite*. Wiley-VCH, New York, 509 pp
- Shalek PD, Petrovic JJ, Hurley GF, Gac FD (1986) *Am Ceram Soc Bull* 65:351
- Sorensen BF (1993) *Scripta Metall Mater* 28:435–439
- Stinton DP, Caputo AJ, Lowden RA (1986) *Am Ceram Soc Bull* 65:347
- Tiegs TN, Becher PF (1986) Tailoring multiphase and composite ceramics. Plenum, New York, p 639
- Urquhart AW (1991) *Mater Sci Eng A* 144:75
- Venkatesh R, Chawla KK (1992) *J Mater Sci Lett* 11:650–652
- Wei GC, Becher PF (1984) *Am Ceram Soc Bull* 64:298

- Wu S, Claussen N (1994) *J Am Ceram Soc* 77:2898
Yang M, Stevens R (1990) *J Mater Sci* 25:4658
Zhu D, Kriven WM (1996) *Ceram Eng Sci Proc* 17:383

Further Reading

- Chawla KK (1998) *Ceramic matrix composites*, 2nd edn. Kluwer, Boston
Colombo P, Riedel R, Sorarù GD, Kleebe H-J (eds) (2009) *Polymer derived ceramics*. Destech, Lancaster, PA
Faber KT (1997) *Annu Rev Mater Res* 27:499
Krenkel W (ed) (2008) *Ceramic matrix composite*. Wiley-VCH, Weinheim
Phillips DC (1983b) Fiber reinforced ceramics. In: Kelly A, Mileiko ST (eds) *Fabrication of ceramics*, vol 4 of *Handbook of composites*. North-Holland, Amsterdam, p 373
Warren R (ed) (1991) *Ceramic matrix composites*. Blackie & Sons, Glasgow

Problems

- 7.1. What are the sources of fiber degradation during processing of ceramic matrix composites?
- 7.2. Describe the advantages of using sol-gel and polymer pyrolysis techniques to process the ceramic matrix in CMCs.
- 7.3. Explain how a carbon fiber reinforced glass-ceramic composite can be obtained with an almost zero in-plane coefficient of thermal expansion.
- 7.4. Chemically, what is an alkoxide? Describe some of the alkoxides that can be used to obtain different ceramic matrixes in CMC.
- 7.5. Distinguish between interphase and interface.
- 7.6. Why is thermal shock resistance more of a problem in CMCs than in MMCs?